



# A review of thermal energy storage technologies and control approaches for solar cooling

Sergio Pintaldi<sup>a,b,\*</sup>, Cristian Perfumo<sup>b</sup>, Subbu Sethuvenkatraman<sup>b</sup>, Stephen White<sup>b</sup>, Gary Rosengarten<sup>a</sup>

<sup>a</sup> School of Aerospace, Mechanical and Manufacturing Engineering, Royal Melbourne Institute of Technology, Melbourne, Australia

<sup>b</sup> Energy Flagship, Commonwealth Scientific and Industrial Research Organisation, Newcastle, Australia

## ARTICLE INFO

### Article history:

Received 1 May 2014

Received in revised form

4 August 2014

Accepted 22 August 2014

### Keywords:

Thermal energy storage

Control strategy

Solar cooling

Solar air-conditioning

Optimization

## ABSTRACT

This paper presents a review of thermal storage media and system design options suitable for solar cooling applications. The review covers solar cooling applications with heat input in the range of 60–250 °C. Special attention is given to high temperature (> 100 °C) high efficiency cooling applications that have been largely ignored in existing reviews. Sensible and latent heat storage materials have been tabulated according to their suitability for double effect and triple effect chillers. A summary of system designs for water storage (sensible heat), and phase change material storage (latent heat) has been provided. The article summarizes literature related to solar thermal air-conditioning systems from a material level as well as plant level considerations. This includes evaluating various control strategies for managing the thermal store, that aid in optimal functioning of a solar air conditioning plant. Modeling approaches are reviewed for sizing the solar thermal store, highlighting the large difference seen in specific storage size when applied in different applications.

© 2014 Elsevier Ltd. All rights reserved.

## Contents

|   |     |
|---|-----|
| 1. Introduction   | 976 |
| 2. Solar cooling system layout and the integration of thermal storage | 976 |
| 3. Examples of solar cooling installations with thermal storage       | 977 |
| 3.1. Systems based on STES  | 977 |
| 3.2. Systems based on LHTEs   | 979 |
| 4. Storage media for solar cooling                                    | 979 |
| 4.1. Sensible heat materials  | 980 |
| 4.1.1. Methods and parameters for material selection                  | 980 |
| 4.1.2. Materials  | 981 |
| 4.2. Latent heat Materials  | 981 |
| 4.2.1. Material selection process                                     | 981 |
| 4.2.2. Thermal conductivity enhancement techniques                    | 982 |
| 4.2.3. PCMs for solar cooling applications                            | 983 |
| 4.3. Thermo-chemical Materials  | 983 |
| 5. Thermal storage system design                                      | 984 |
| 5.1. Active TESS using water as storage media                         | 985 |
| 5.1.1. Stratification improvements                                    | 986 |
| 5.2. Latent heat applications   | 987 |
| 5.3. High temperature solar thermal applications                      | 987 |
| 6. Control approaches for solar cooling systems                       | 989 |
| 6.1. Advanced model-based and look-ahead control approaches           | 989 |

\* Corresponding author at: School of Aerospace, Mechanical and Manufacturing Engineering, Royal Melbourne Institute of Technology, Melbourne, Australia.  
Tel.: +61 2 4960 6261; fax: +61 2 4960 6021.

E-mail address: [sergio.pintaldi@csiro.au](mailto:sergio.pintaldi@csiro.au) (S. Pintaldi).

|   |     |
|---|-----|
| 6.2. Summary .....  | 991 |
| 7. Design process approaches for thermal storage system selection for solar cooling ..... | 991 |
| 8. Conclusion .....   | 992 |
| Acknowledgments .....   | 993 |
| References .....  | 993 |

## 1. Introduction

Solar thermal cooling systems convert incident solar radiation into heat (through solar thermal collectors) and use this heat to generate cooling through a thermally activated cooling device such as an absorption or adsorption chiller, desiccant system or ejector refrigeration system. There is growing interest in solar cooling and an increasing number of installations around the world [1–3].

Unfortunately, solar energy is an intermittent resource. While solar photovoltaic technology is becoming increasingly cost effective at producing electrical energy, it cannot provide “firm” power without the extra cost of battery storage. Consequently, when aiming for a predominantly solar powered electricity grid, system planners must consider the full cost of both (i) energy supply and (ii) diurnal matching with demand, including the resulting extra cost of storage.

In warm climates, where air-conditioning is responsible for a large fraction of greenhouse gas emissions and dominates peak electricity demand [4], solar cooling offers an alternative approach for both reducing emissions and managing solar intermittency. In particular, solar thermal cooling technology offers a much cheaper approach for storing energy, leading to reduced overall system cost.

Just as the low cost of thermal storage is a key justification for concentrating solar power in the wholesale electricity market, low cost thermal storage may prove a key benefit for managing energy flows in the retail electricity market. The use of thermal storage, in a solar cooling system, can also increase the fraction of the total building energy consumption that can be supplied by solar [1,5–7].

This article presents a review of thermal storage media, system design options and controls suitable for solar cooling applications.

Though there have been review papers pertaining to thermal energy storage, they mainly focussed on storage media and heat exchanger design aspects of a solar cooling system [8–10]. There is also a wealth of literature available on thermal storage for solar thermal power generation systems (e.g. [11]).

However, none of these reviews have sufficiently documented the integration aspects of a thermal storage system in the solar cooling plant design, or covered the system control approaches required for managing charging and discharging of the thermal

store in order to maximize cooling output and achieve robust operation.

In addition to covering these thermal storage integration issues, this review focuses significantly on thermal storage for high efficiency double effect and triple effect absorption chillers. This is a more recent area of solar cooling research with the potential for improving the overall economics of solar thermal cooling systems, because high chiller efficiency can potentially enable solar collector area to be reduced. White and Goldsworthy [12] highlight the importance of high efficiency chillers as the only way to actually increase the value of collected solar heat, compared with just using the solar heat (as is for hot water or space heating) without further conversion to cooling. However thermal storage becomes more problematic in these systems because expensive pressure vessels are required when using water as the thermal storage medium.

## 2. Solar cooling system layout and the integration of thermal storage

A typical solar cooling system with an absorption chiller is represented in Fig. 1.

This generic solar thermal cooling system consists of two flow loops separated by the hot thermal storage component. A solar heating flow loop conveys heat from solar thermal collectors to the thermal store. A thermal cooling flow loop conveys heat from the thermal store to the thermal cooling device. When the heat arriving from the collectors exceeds the heat being consumed by the thermal cooling device, then the thermal store is charged. Conversely, when the demand for heat to the thermal cooling device exceeds the supplied solar heat, the thermal store is discharged to match demand.

The storage medium in the thermal store, can store heat in the form of either (i) sensible heat, (ii) latent heat (that involves a phase change of storage material) or (iii) in the form of reversible physio-chemical reactions. Factors such as energy storage density, operating temperature, mechanism of heat exchange and cost play

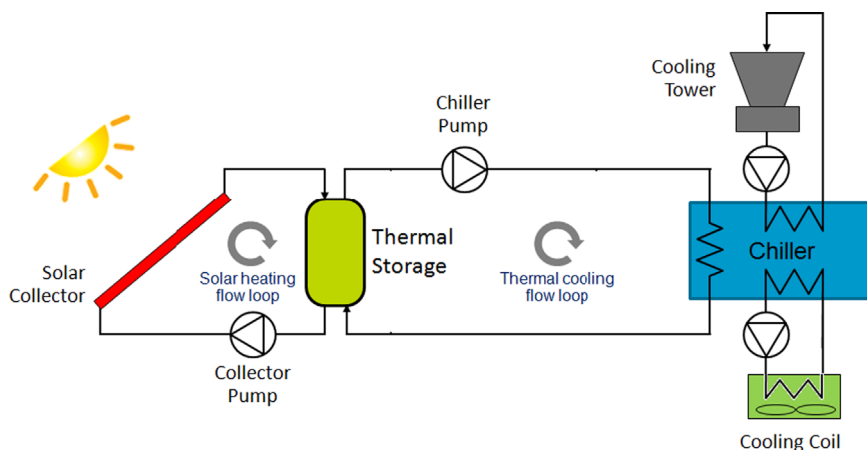


Fig. 1. A generic solar thermal cooling system [13].

a major role in the economic down-selection of a suitable storage medium. Storage medium selection is discussed in more detail in Section 4.

In most solar cooling installations to date (see Section 3), the thermal store uses a sensible heat storage medium which is one and the same as the liquid heat transfer fluid in either or both of the two flow loops. The simultaneous collection, transfer and storage of heat is termed *direct* thermal storage. *Indirect* thermal storage system involves a separate storage medium from the collector heat transfer fluid, incorporating some form of heat exchange arrangement [14].

It is clear that the operation and performance of the thermal store is highly integrated with the process flow arrangement/design of the full solar cooling system. This can be seen in the operating temperature of the thermal store, which will depend on the thermal cooling device. For example, absorption chillers are divided into three categories based on the temperature of heat input required to drive them.

- (1) Single-effect absorption chillers: hot source inlet temperature range of 65–95 °C
- (2) Double-effect absorption chillers: hot source inlet temperature range of 155–185 °C
- (3) Triple-effect absorption chillers: hot source inlet temperature > 200 °C

The operating temperature of the chiller is clearly a key criterion when selecting the solar collector and a suitable storage material for solar cooling systems. As a result there are many variations to the generic solar thermal cooling flow scheme illustrated in Fig. 1, based largely on materials selection issues. For example, frost protection may require an additional flow loop between the thermal store and the externally mounted solar thermal collectors. Or the potential for high pressures may make it attractive to use low volatility heat transfer fluids in a separate atmospheric pressure flow loop.

Additional flow loops require additional heat exchangers, external or internal to the thermal store. Heat exchange selection is discussed in more detail in Section 5.

A range of application constraints/alternatives may also influence the layout, including the optional addition of potable hot water production and the optional use of gas as a backup heat source. A schematic representation approach for categorizing the large number of possible variants was developed by Becker et al. [15], an example of which is illustrated in Fig. 2.

### 3. Examples of solar cooling installations with thermal storage

Numerous solar air-conditioning systems are in commercial operation. According to published information, the number of solar heating and cooling systems in the EU region is estimated to be around 100 [16,17]. Preisler [2] has compiled a list of solar cooling and heating systems in 2009. Mugnier and Jakob [3] suggest there may be as many as one thousand systems installed. Most of these systems are single stage absorption chillers using water as the working fluid.

This section reviews published information on practical solar cooling installations, categorized into systems with Sensible heat based Thermal Energy Storage (STES) and Latent Heat based Thermal Energy Storage (LHTES) systems.

#### 3.1. Systems based on STES

Table 1 provides a snapshot of installations of solar cooling systems that use sensible heat storage media. These examples have been chosen to represent various solar collectors used in these applications in last 10 years. The following abbreviations are used: SE for single-effect, DE for double effect absorption chillers, FPC for flat-plate, ETC for evacuated tube, PTC for parabolic trough, CPC for compound parabolic concentrator and LFC for Linear Fresnel Concentrating collectors.

It can be seen that single effect absorption chillers have used non concentrating solar heat collection methods and double effect chillers have used concentrating heat collection methods. In some cases no storage is included in the solar cooling plant.

Use of solar heat input to triple effect chillers is very scarce. Recently researchers from Kawasaki published a paper exploring the benefits of a steam driven triple effect chiller operated with

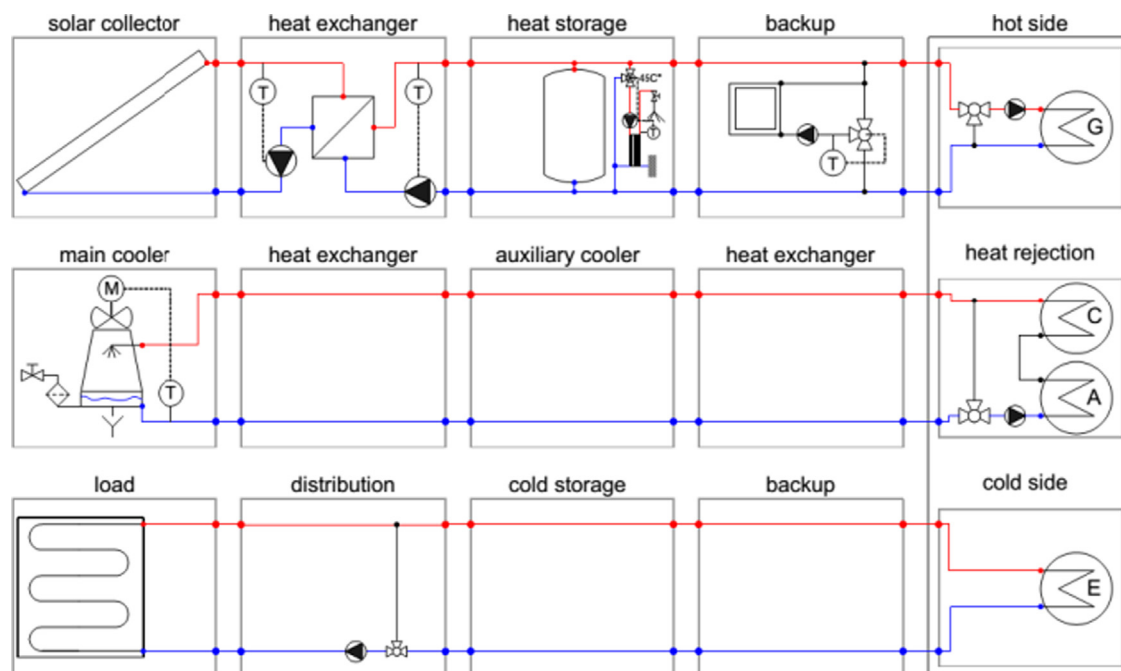


Fig. 2. Solar absorption cooling system [15].

**Table 1**

Summary of literature on solar cooling systems with sensible thermal storage.

| Chiller details         | Heat collection system                 | Solar collector heat transfer fluid (SCHTF)          | Chiller heat transfer fluid (CHTF) | Thermal storage media   | TES system/method   | Chiller hot source temperature range | Conclusions/Findings/Features/type of study  | Ref. |
|-------------------------|--|--|------------------------------------|-------------------------|---|--------------------------------------|--|------|
| 35 kW <sub>c</sub> SE   | 50 m <sup>2</sup> FPC                  | Water (+ propylene glycol)                           | Water                              | Water                   | 2 m <sup>3</sup> stratified hot water storage/indirect                        | 65–90 °C                             | The use of a storage buffer (i) extended the daily cooling period, (ii) gave higher system efficiency and (iii) prevented cycling of the absorption chiller due to variations of the solar radiation   | [21] |
| 35 kW <sub>c</sub> SE   | 151 m <sup>2</sup> FPC                 | Water  | Water                              | Water                   | 2500 l two tanks working in parallel/direct                                   | 75–100 °C                            | Development of a dynamic model for a demonstration solar cooling plant. The model resulted validated with a 3% tolerance on the energy balance. The model allowed checking the correct operation of the systems. The simulations indicated that the better system performance is obtained when the chiller generator power is more stable. | [22] |
| 35.2 kW <sub>c</sub> SE | 72 m <sup>2</sup> ETC                  | Water  | Water                              | Water                   | 400 l hot water tank+200 l cold water storage/direct                          | 70–95 °C                             | LPG fired heating unit in parallel with the storage tank. The installation demonstrated the potential of solar cooling, compared to conventional chillers, in providing environmentally friendly air-conditioning.   | [23] |
| 35 kW <sub>c</sub> SE   | 108 m <sup>2</sup> ETC                 | Water + anti-freeze                                  | Water                              | Water                   | 6.8 m <sup>3</sup> hot water tank+1.5 m <sup>3</sup> cold water tank/indirect | 50–90 °C                             | In the cold tank, the cold can be either provided by the chiller evaporator or by free cooling, obtained from the cooling tower  | [24] |
| 4.5 kW <sub>c</sub> SE  | 37.5 m <sup>2</sup> FPC                | n.a.   | Water                              | Water                   | 700 l stratified tank/indirect  | n.a.                                 | Storage does not operate in the normal system operation: the dynamic simulations evaluated new control strategies to operate the storage   | [25] |
| 70 kW <sub>c</sub> SE   | 162 m <sup>2</sup> FPC                 | Water  | Water                              | Water                   | Two stratified 5000 l storage tanks/direct                                    | 70–95 °C                             | The authors emphasized the role of the storage in providing heat not only in radiation unavailability period but also in the start-up moments in the morning.  | [26] |
| 70 kW <sub>c</sub> SE   | 108 m <sup>2</sup> ETC                 | Water + 35%wt propyleneGlycol                        | Water                              | Water                   | 8 × 51.5 m <sup>3</sup> Concrete tanks/indirect                               | 70–95 °C                             | The stratification is achieved using linear diffusers for both hot water inlet and cold water outlet: water mixing is avoided due to low flow velocity and uniform temperature flow in and out of the tank   | [27] |
| 10 kW <sub>c</sub> SE   | 105 m <sup>2</sup> CPC-ET              | Water  | Water                              | Water                   | Hot water tank/n.a.   | n.a.                                 | The study focused on the comparison of two systems: adsorption and absorption coupled with CPC collectors. No detailed information on the TES system has been found.   | [28] |
| 70 kW <sub>c</sub> DE   | 106.5 m <sup>2</sup> Integrated CPC-ET | Pressurized water                                    | Pressurized water                  | Pressurized water       | Insulated 3900 l horizontal steel tank/direct                                 | 150 °C                               | The work does not report further information on the TES, since it is focused on the collector and chiller performance  | [29] |
| DE                      | 360 m <sup>2</sup> PTC                 | Pressurized water                                    | Pressurized water                  | Pressurized water       | 6 m <sup>3</sup> hot water tank+ Chilled water tank/direct                    | 155–180 °C                           | Demonstration of the advantages of steam fired DE absorption chillers coupled with PTC.  | [30] |
| 16 kW <sub>c</sub> DE   | 52 m <sup>2</sup> PTC                  | Pressurized solution of water+ 50%wt propyleneGlycol | n.a.                               | None                    | None  | 140–160 °C                           | Smallest high temperature solar cooling system in the world at that stage. Simulation included a storage in order to investigate its benefits. The storage tank did not improve the system performance of solar cooling. The study provided guidelines for future designs.   | [31] |
| 16 kW <sub>c</sub> DE   | 40 m <sup>2</sup> PTC                  | Thermal oil  | Thermal oil                        | Thermal oil             | 400 l drainback tank+200 l Buffer/direct                                      | 150–160 °C                           | The storage tank did not improve the system performance of solar cooling. The installation of the new 400 l drainback tank to avoid start-up delays of chiller due to radiant heat losses of the HTF in the night, lead to increasing the solar fraction of the system from 0.54 to 0.77   | [32] |
| 25 kW <sub>c</sub> DE   | LFC                                    | Pressurized water/steam                              | Pressurized water                  | Pressurized water/steam | Steam drum + Feed water tank; 1200 l ice storage/(in) direct.                 | 140–200 °C                           | Different control strategies and chiller operation modes investigated.   | [33] |
| 16 kW <sub>c</sub> 2xDE | 30 m <sup>2</sup> External CPC-ET      | Pressurized water                                    | Steam or water/natural gas         | None                    | None  | n.a.                                 | The solar heating and cooling plant is located at Carnegie Mellon University. Two absorption chillers are installed: steam fired and hot water/natural gas fired. The study regards the exergy analysis of the system with the hot water fired machine. No storage is mentioned.   | [34] |
| 174 kW <sub>c</sub> DE  | 352 m <sup>2</sup> LFC                 | Pressurized water                                    | Pressurized water                  | None                    | None  | n.a.                                 | The article focused on the operational behavior of the cooling plant installed at University of Seville. No storage is installed; the heat demand is balanced by mean of a direct-fired natural gas burner.  | [35] |

solar heat [18]. Thermax [19] has installed a triple effect absorption chiller powered by trough collectors at the solar energy center in India. Storage aspects of these triple effect absorption chiller installations are not available in the literature at the present stage.

Sparber et al. [20] reviewed the volume of storage installed in a sample of installations in the IEA Solar Heating and Cooling Programme “Solar Airconditioning and Refrigeration” Task38. Based on the findings illustrated in Fig. 3, they found that there was no

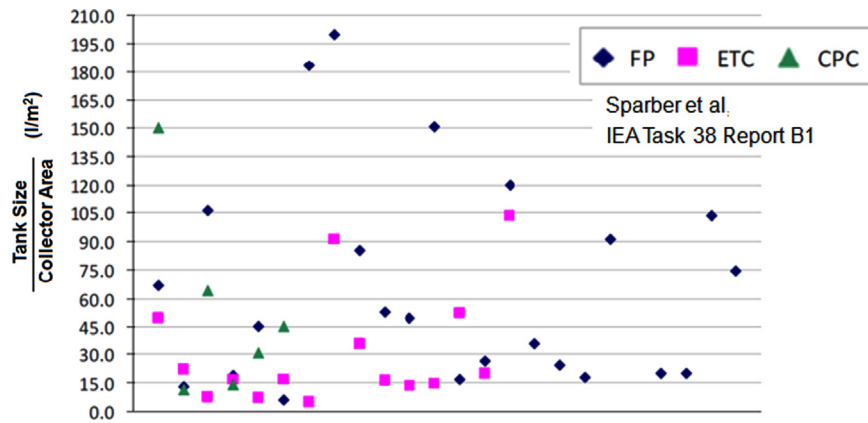


Fig. 3. Tank to collector area ratio for different types of collectors (FPC, ETC, CPC) of 46 solar cooling installations, adapted from [20].



Fig. 4. Latent heat thermal energy storage image and characteristics for a storage system installed in Seville, Spain [39].

|                                | Units | Values |
|--------------------------------|-------|--------|
| Diameter of the tank           | [mm]  | 900    |
| Length of the tank             | [mm]  | 7400   |
| Number of tubes                | [-]   | 330    |
| Length of the tubes            | [mm]  | 6000   |
| External diameter of the tubes | [mm]  | 17.2   |
| Internal diameter of the tubes | [mm]  | 13.2   |
| Mass of PCM                    | [kg]  | 4600   |

consistent trend in the volume of storage employed in solar airconditioning installations.

This probably reflects (i) the diversity of applications to which the solar cooling system is being applied (e.g. whether or not domestic hot water is being produced from the system) and (ii) the relative sizing of collector area and chiller size. A large collector area with small chiller is likely to have spare solar heat available to be stored, whereas an undersized collector field (relative to the chiller) will use up all available solar heat when its available leaving nothing to be stored.

In any case, some amount of storage will be required, as a minimum, to ensure stable operation of the chiller and prevent rapid start-up/ shut-down events. This is particularly important with absorption chillers which have relatively slow start up times ( $\sim 30$  min) due to high thermal mass, and a dilution cycle when shut down.

### 3.2. Systems based on LHTES

There are only a small number of latent heat storage examples being used in solar air-conditioning applications. Laboratory prototypes for LHTES for solar heating and cooling have been investigated as a part of IEA solar heating and cooling task force (task 32) [36]. They found that the storage density, in comparison with water, is strongly dependent on the temperature lift (temperature difference between tank top and bottom) in the storage tank.

At the University of Lleida, Spain, a laboratory pilot plant has been built in order to test different TESSs and materials [37–39] for high temperature solar air-conditioning applications with double effect absorption chillers. The facility is composed of three components: heating system, storage and cooling system. For test purposes, an electrical boiler (24 kW<sub>e</sub>) and a dry cooler (20 kW<sub>e</sub>)

are used to provide heat input and remove the heat from the storage system in place of the solar collector and absorption chiller respectively.

This facility was used to compare the performance of hydroquinone and D-mannitol as latent heat storage materials with phase change around 170 °C. In contrast to the hydroquinone material, tests showed that undesirable sub-cooling (below the material freezing temperature) occurred for D-mannitol during the heat store discharge cycle. Tests also explored the impact of two different thermal store heat exchange designs based on finned and un-finned shell-and-tube TES [38].

Based on these laboratory results, a 17.6 kW PCM storage tank was designed and built to work in a real solar cooling plant in Seville, Spain [39]. It was installed as part of the solar refrigeration installation on the roof of the Engineering School building at University of Seville (Fig. 4). Its main function is to provide heat to the solar cooling system during periods of radiation unavailability. The design consists of a cylindrical vessel with a tube bundle inside. The heat transfer fluid is circulated inside the tubes, organized in a triangular pitch, while the PCM is located in the outer tube part, the housing.

## 4. Storage media for solar cooling

The storage medium can store heat in the form of sensible heat, latent heat (that involves a phase change of storage material) or in the form of reversible physio-chemical reactions. While sensible storage dominates existing installations, the incentive for other forms of thermal energy storage is the reduction in volume required for the thermal store. Fig. 5 illustrates the indicative effect of storage material choice on the TES system volume when storing 10 MJ of heat [5].



Identification of a suitable material for a given application also requires evaluation of a range of other thermo-physical, and chemical properties of candidate materials. This section provides a summary of storage material related research suitable for solar cooling applications.

#### 4.1. Sensible heat materials

The amount of energy transferred to the storage media in a sensible heating process is proportional to the difference between the storage material's final and initial temperatures, the mass of the storage medium and its heat capacity [40]. Sensible storage can be in the form of (i) a solid material being indirectly heated and cooled by a heat transfer fluid or (ii) a liquid material contained in a storage tank.

##### 4.1.1. Methods and parameters for material selection

The selection of sensible heat storage materials can be made by qualitatively comparing relevant parameters of materials in a table [11]. Relevant parameters for evaluation of sensible heat storage media are listed below.

- Specific heat capacity (kJ/kgK): It indicates the material ability to store thermal energy for a given mass.
- Volumetric heat capacity (kJ/m<sup>3</sup>K): material's ability to store thermal energy for a given volume.
- Thermal conductivity (W/mK): It indicates the material ability to rapidly transfer heat. This is important during indirect heat transfer based thermal storage systems.
- Cost per unit of energy (\$/kWh or \$/kJ): It indicates the cost of the material for storing one unit of heat energy in a given thermal store.

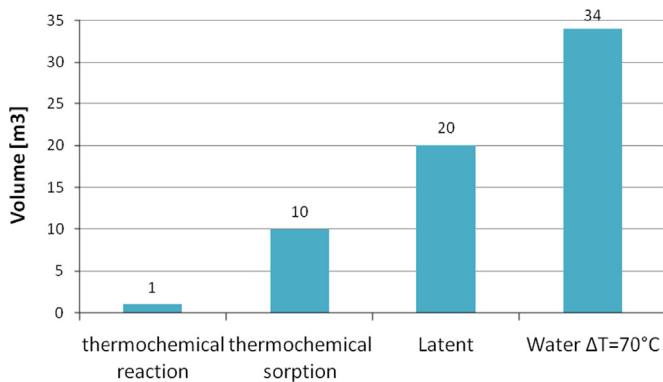


Fig. 5. Comparison of the different types of materials for TES, adapted from [5].

**Table 2**  
Sensible heat materials for solar cooling applications.

| Physical properties                            | Synthetic Oil | Water @20 °C | Reinforced concrete | Sand-rock-mineral oil | NaCl solid | Cast iron | Silica fire bricks | Magnesia fire bricks |
|--|---------------|--------------|---------------------|-----------------------|------------|-----------|--------------------|----------------------|
| Specific heat capacity (kJ/kgK)                | 2.3           | 4.182        | 0.850               | 1.300                 | 0.850      | 0.560     | 1.000              | 1.150                |
| Mass density (kg/m <sup>3</sup> )              | 900           | 1000         | 2200                | 1700                  | 2160       | 7200      | 1820               | 3000                 |
| Thermal conductivity (W/mK)                    | 0.11          | 0.58         | 1.5                 | 1                     | 7          | 37        | 1.5                | 1                    |
| Volumetric heat capacity (kJ/m <sup>3</sup> K) | 2070          | 4182         | 1870                | 2210                  | 1836       | 4032      | 1820               | 3450                 |
| Cost ratio <sup>a</sup>                        | 3261          | 1            | 54                  | 163                   | 163        | 1087      | 1087               | 2174                 |
| Cost (USD/kWh)                                 | 117.4         | 0.02         | 5.3                 | 10.4                  | 15.9       | 160.7     | 90.0               | 156.5                |
| Energy density ratio <sup>b</sup>              | 0.49          | 1.00         | 0.45                | 0.53                  | 0.44       | 0.96      | 0.43               | 0.82                 |
| Reference                                      | [11]          | [45,46]      | [11,47]             | [11,47]               | [11,47]    | [11,47]   | [11,47]            | [11,47]              |

<sup>a</sup> The cost assumed for water is  $0.92 \times 10^{-3}$  USD/kg [46].

<sup>b</sup> The energy density has been evaluated considering a temperature difference of 40 °C of an ideal thermal process relative to water.

All those parameters can be used for a “first” evaluation of the material to be used in a TES.

Fernandez et al. [41] presented a method to select materials for sensible heat storage applications. The case study took into account a temperature range between 150 and 200 °C and two different scenarios were considered: long-term (storage for weeks/months) and short-term (storage for hours/days) storage. The authors analyzed possible materials using a commercial software package (CES Selector). The selection process took into consideration four aspects:

- Function of the component for which the material is sought (e.g. long-term storage purposes).
- List of constraints that must be met by the material (e.g. limits on minimum storage density, temperature limit, thermal conductivity).
- List of optimization objectives to judge the material effectiveness (e.g. cost).
- List of free variables, the ones chosen by the designer (e.g. dimensions of material).

The objective of the optimization, in long term storage systems, was to maximize the energy stored per unit of material cost as well as the thermal conductivity. The free variables were the material choice and storage dimensions. The authors also introduced an upper limit for the specific cost of the materials as 5€/kg. They optimized the energy density per unit cost ( $Q_{dens}$ ) given as below

$$Q_{dens} = \frac{c_p \Delta T}{V C_m} \quad (1)$$

Here  $\Delta T$  is the difference in temperature between the storage and the process,  $V$  the volume and  $C_m$  the cost per mass unit of the material. The term  $c_p/C_m$  is related only to the material properties. That is defined as the material index: the materials with the same index will perform equally.

In the case of short-term storage systems, the function to be optimized is the maximization of the energy stored for a given temperature rise, time and material thickness. The thermal diffusivity is introduced as an indirect measure of the time. In the case of short-term storage materials, the formulation of the equation to be optimized is

$$C = A \sqrt{2\tau a^{1/2} \rho C_m} \quad (2)$$

Where  $A$  is the area of the material,  $\tau$  the time,  $a$  the thermal diffusivity,  $\rho$  the material density and  $C_m$  the specific cost of the material. In this case the material index is given by

$$M = \frac{1}{a^{1/2} \rho C_m} \quad (3)$$

The authors found that sodium chlorite (halite) had the lowest cost per unit of thermal energy stored for long term storage. Ceramic materials like concrete or supersulphate cement or sodium chloride (NaCl) had the lowest cost per unit of thermal energy stored for the short-term storage.

#### 4.1.2. Materials

The most common material used in a sensible heat storage system is water [42]. High specific heat capacity, wide availability, chemically stability and low cost make water a good storage media suitable for low temperature solar cooling applications (e.g. single stage absorption chillers and desiccant systems). Due to the boiling point constraint (100 °C at 1 bar), use of water as sensible heat storage medium for high temperature application (double effect and triple effect chillers) requires increasing the system pressure. For example, triple effect chillers operating with 200 °C heat input might need the storage vessel and the piping to be designed for 35 bar to handle water in liquid state.

Laing et al. [43] investigated the performance of two solid media in high temperature heat storage for solar power plants. Both concrete and castable ceramics materials were found to be suitable for the application. Concrete is particularly attractive due to its lower cost, higher strength and easier handling. In the report compiled by the NREL [44] a wide choice of materials suitable for high temperature solar power plants is summarized together with the experience of previous thermal energy storage systems applied to solar parabolic trough power plants. A summary of sensible storage materials suitable for solar cooling applications is provided in Table 2. The materials have been selected by energy density and cost considerations (below 5 USD/kg).

Though salts are primarily used in phase change applications, salts in molten form are also a potential candidate for sensible heat

storage. They are attractive due to their low cost. A summary of other potential sensible heat storage materials are listed in Table 3. The materials have been selected with an energy density ratio higher than 0.5. The only exemption is sandstone due to its high thermal conductivity. No information on the cost has been found in the source.

Materials that have energy density values similar to water (e.g. asphalt sheet) could be a potential candidate for high temperature (> 100 °C) storage.

In conclusion, it can be stated that for single effect chiller applications, water is the most suitable candidate due to its thermal properties and cost. For double effect and triple effect applications, materials such as synthetic oil, concrete and asphalt could be potential choices. The final choice would be guided by thermal storage system design, cooling system requirements and economic constraints.

#### 4.2. Latent heat Materials

These materials store heat associated with phase transition. The amount of heat stored in these materials is proportional to the material mass, the fraction of material that undergoes the phase change, and the material heat of fusion. The materials used in latent heat storage are also known as phase change materials (PCM). The phase change can take place in various ways: solid–solid, solid–liquid, solid–gas and liquid–gas. The first case is related to storing heat by transition between different kinds of crystallization forms and is characterized by a relative low latent heat and small volume changes compared to the others [8]. The solid–gas and liquid–gas transitions are associated with a big volume changes leading to system complexity and containment problems, hence they are not suitable in TES applications. Although the solid–liquid phase change has relatively lower latent heat compared to the liquid–gas ones, their change in volume is smaller. Hence they have been widely studied in past years [44,49,50]. Phase change materials used in latent heat thermal energy storage can be divided into three categories [8]: organic, inorganic and eutectic. In practical applications, the most widespread materials are paraffins (organics), hydrated salts (inorganics) and fatty acids (inorganics) [8]. However the use of metal alloys could provide a solution to the low thermal conductivity of solid organics and salts [51].

##### 4.2.1. Material selection process

Sharma et al. [8] summarized the characteristics of PCMs suitable in thermal storage applications. These include, (i) a suitable phase change temperature, (ii) good thermal conductivity, (iii) small volume change during the phase change process, (iv) chemical stability, (v) safety, and (vi) cost effectiveness. The material selection

**Table 3**  
Additional sensible heat materials with good thermal properties [48].

| Materials      | Energy density ratio <sup>a</sup> | Thermal conductivity (W/mK) | Materials      | Energy density ratio <sup>a</sup> | Thermal conductivity (W/mK) |
|----------------|-----------------------------------|-----------------------------|----------------|-----------------------------------|-----------------------------|
| Granite        | 0.57                              | 2.90                        | Aluminum       | 0.58                              | 204                         |
| Marble         | 0.52                              | 2.00                        | Aluminum oxide | 0.78                              | 30                          |
| Sandstone      | 0.37                              | 1.83                        | Isobutanol     | 0.58                              | 0.13                        |
| Asphalt sheet  | 0.93                              | 1.20                        | Pure iron      | 0.85                              | 73                          |
| Steel slab     | 0.94                              | 20                          | Copper         | 0.82                              | 385                         |
| Asbestos sheet | 0.63                              | 0.16                        | Stone, granite | 0.52                              | 1.7–3.98                    |

<sup>a</sup> The energy density has been evaluated considering a temperature difference of 40 °C of an ideal thermal process relative to water.

| Material             | Literature data               |  | Experimental data by DSC          |  |
|----------------------|-------------------------------|--|-----------------------------------|--|
|                      | Phase change temperature [°C] | Phase change enthalpy [kJ kg <sup>-1</sup> ] | Phase change temperature [°C]     | Phase change enthalpy [kJ kg <sup>-1</sup> ] |
| Salicylic acid       | 159                           | 199  | 159.1 (m) <sup>a</sup> /111.3 (s) | 161.5  |
| Benzanilide          | 161                           | 162  | 163.6 (m)/136.1 (s)               | 138.9  |
| d-mannitol           | 167                           | 316  | 166.8 (m)/117 (s)                 | 260.8  |
| Hydroquinone         | 172.4                         | 258  | 172.5 (m)/159.5 (s)               | 225  |
| Potassium thiocynate | 173                           | 280  | 176.6 (m)/156.9 (s)               | 114  |

a (m) melting and (s) solidification.

**Fig. 6.** Comparison of the thermal properties of selected PCMs [39].

**Table 4**  
Phase change materials for single-effect absorption and desiccant solar cooling systems.

| Material   | Melting point (°C) | Heat of fusion (kJ/kg) | Specific heat capacity liq./sol. (kJ/kgK) | Thermal conductivity (W/mK)          | Density liq./sol. (kg/m <sup>3</sup> ) | Cost (USD/kg) | Type as in ref. [8] | Ref.       |
|--|--------------------|------------------------|---|--------------------------------------|--|---------------|---------------------|------------|
| RT65 (Rubitherm) <sup>a</sup>                              | ≈ 64               | ≈ 154/173              | 2.4/1.8                                   | 0.2                                  | 790/910 (70/15 °C)                     | 4.0–4.8       | Org. par.           | [53,55]    |
| RT81 (Rubitherm) <sup>a</sup>                              | ≈ 81               | ≈ 140                  | 2.4/1.8                                   | 0.2                                  | 770/920 (100/15 °C)                    | 4.0–4.8       | Org. par.           | [53]       |
| PK80 A6 (Rubitherm) <sup>a</sup>                           | ≈ 81               | ≈ 119                  | 2   | 0.2                                  | 900 (20 °C)                            | 8.2           | Org. par.           | [53]       |
| TH89 (TEAP energy) <sup>b</sup>                            | 89                 | 139.6/149              | 2.83/1.84                                 | 0.60/0.69 (110/140 °C)               | 1640 (25 °C)                           | 9 (100 kg)    | n.a.                | [53,55]    |
| Mg(NO <sub>3</sub> ) <sub>2</sub> · 6H <sub>2</sub> O      | 89.3–89.9          | 149–175                | 1.84/2.51                                 | 0.57 (120 °C) 0.490/0.669 (95/56 °C) | 1550/1636 (94/25 °C)                   | 3             | Inorg. salt hyd.    | [53,54,56] |
| RT90 (Rubitherm) <sup>a</sup>                              | ≈ 90               | ≈ 163/194              | 2.4/1.8                                   | 0.2                                  | 770/930 (100/15 °C)                    | 4.0–4.8       | Org. par.           | [53,55]    |
| Xylitol C <sub>5</sub> H <sub>7</sub> (OH) <sub>5</sub>    | 93–94.5            | 263.3                  | n.a.                                      | n.a.                                 | 1520 (20 °C)                           | 6.7–8.3       | Org. sug. alc.      | [53]       |
| D-sorbitol C <sub>6</sub> H <sub>8</sub> (OH) <sub>6</sub> | 96.7–97.7          | 185                    | n.a.                                      | n.a.                                 | 1500 (20 °C)                           | 1.1           | Org. sug. alc.      | [53]       |

<sup>a</sup> Conversion assumed 1 EUR = 1.37 USD (20/02/2014)

<sup>b</sup> Conversion assumed 1 AUD = 0.90 USD (20/02/2014)

**Table 5**  
Phase change materials for double-effects absorption solar cooling systems.

| Material   | Phase change point (°C) | Heat of fusion (kJ/kg) | Density liq./sol. (kg/m <sup>3</sup> ) | Type as in ref. [8] | Ref. |
|--|-------------------------|------------------------|--|---------------------|------|
| Alpha glucose  | 141                     | 174                    | 1544                                   | Org. sug. alc.      | [55] |
| NaNO <sub>2</sub> (40 wt%)+NaNO <sub>3</sub> (7 wt%)+KNO <sub>3</sub> (53 wt%) | 142                     | n.a.                   | n.a.                                   | Eut. inorg.         | [55] |
| Acetyl-p-toluidene   | 146                     | 180                    | n.a.                                   | Org. sug. alc.      | [55] |
| 2,2-Bis(Hydroxymethyl) Propionic acid <sup>a</sup>                             | 152                     | 289                    | n.a.                                   | Org. non par.       | [55] |
| Phenylhydrazine benzaldehyde   | 155                     | 134.8                  | n.a.                                   | Org. sug. alc.      | [55] |
| Salicylic acid   | 159                     | 199                    | 1443 (20 °C)                           | Org. sug. alc.      | [55] |
| Benzanilide  | 161                     | 162                    | n.a.                                   | Org. sug. alc.      | [55] |
| E164 (EPS Ltd)   | 164                     | 306                    | 1500                                   | n.a.                | [53] |
| O-Mannitol   | 166                     | 294                    | 1489 (20 °C)                           | Org. sug. alc.      | [55] |
| D-mannitol   | 166–168                 | 316.4                  | 1520 (20 °C)                           | Org. sug. alc.      | [53] |
| 38.2%NPG/61.8%PE <sup>a</sup>  | 170                     | 147                    | n.a.                                   | Org. non par.       | [55] |
| Hydroquinone   | 172.4                   | 258                    | 1358 (20 °C)                           | Org. sug. alc.      | [55] |
| Penterythritol (PE) <sup>a</sup>   | 185                     | 303                    | n.a.                                   | Org. non par.       | [55] |
| p-Aminobenzoic acid  | 187                     | 153                    | n.a.                                   | Org. sug. alc.      | [55] |
| Galactitol   | 188–189                 | 351.8                  | 1470 (20 °C)                           | Org. sug. alc.      | [53] |

<sup>a</sup> Solid–solid PCM

process for latent heat materials can be illustrated using the approach adopted by Gil et al. [52]. The authors designed a thermal energy storage system for a solar cooling plant with a two stage absorption chiller. The first criterion was the temperature range: the operating temperature of the solar cooling system for the double effect absorption chiller was required to be between 140 and 200 °C, where the latter was the maximum collector outlet temperature. The second decision parameter was the heat of fusion: A heat of fusion higher than 150 kJ/kg was chosen as a baseline for comparison. Then the authors compared different materials, by a literature review and through experimental studies, and compiled a table (Fig. 6) with the best candidates. D-mannitol and hydroquinone were selected through this process.

#### 4.2.2. Thermal conductivity enhancement techniques

A typical issue with many phase change materials is low thermal conductivity e.g. solar salt (KNO<sub>3</sub>/NaNO<sub>3</sub>). Where thermal conductivity is low, the outside solid layer formed during heat

discharge can form an insulating barrier preventing heat transfer from the inner molten PCM undergoing solidification.

The possibilities to enhance thermal conductivity are summarized by Fernandes et al. [47]. These include:

- Use of metal structures made of steel or stainless steel that act like a carrier
- Dispersion of high conductivity material, e.g. copper, silver or aluminum particles within the PCM
- Use of high conductivity and low density materials like carbon fibres and paraffin composites
- Impregnation of high conductivity porous materials: metal foam (copper, steel or aluminum) or porous material like graphite.

The authors compared different methods and found, from a cost, handling and availability point of view, that the metal foam technique is the most promising and suitable approach to enhance the thermal conductivity of a PCM,



**Table 6a**

Phase change materials for triple effect absorption chiller based solar cooling systems.

| Material                                       | Melting point (°C) | Energy density (kWh/m <sup>3</sup> ) | Specific energy (kWh/kg) | Latent heat of fusion (kJ/kg) | Thermal conductivity (W/mK) | Mass density (kg/m <sup>3</sup> ) | Ref.    |
|--|--------------------|--------------------------------------|--------------------------|-------------------------------|-----------------------------|-----------------------------------|---------|
| 68.1%KCl /31.9% ZnCl <sub>2</sub>              | 235                | 136.4                                | 0.055                    | 198                           | 0.8                         | 2480                              | [59]    |
| Solar salt KNO <sub>3</sub> /NaNO <sub>3</sub> | 220                | 53.7                                 | 0.028                    | 100.7                         | 0.56                        | 1920                              | [60]    |
| Sn   | 232                | 119.8                                | 0.016                    | 59                            | 66.8                        | 7365/6990(25/232°C)               | [57,61] |
| Al–Sn  | 232                | 119.4                                | n.a.                     | 59                            | 237                         | n.a.                              | [51]    |
| Inv Struct Al–Sn                               | 232                | 41.9                                 | n.a.                     | n.a.                          | n.a.                        | n.a.                              | [51]    |
| 4-Hydroxy benzoic acid                         | 213                | 90.9                                 | 0.062                    | 223.7                         | n.a.                        | 1463                              | [57]    |
| Propazine                                      | 217                | 58.8                                 | 0.051                    | 182.3                         | n.a.                        | 1162                              | [57]    |
| N,N'-Diphenylurea                              | 236                | 56.1                                 | 0.045                    | 163                           | n.a.                        | 1239                              | [57]    |
| Caffeine                                       | 236.1              | 38.8                                 | 0.031                    | 113.3                         | n.a.                        | 1232                              | [57]    |
| Indium(I) chloride                             | 225                | 71.2                                 | 0.017                    | 61.2                          | n.a.                        | 4190                              | [57]    |
| Metaboric acid (γ form)                        | 236                | 225.4                                | 0.091                    | 326.3                         | n.a.                        | 2487                              | [57]    |
| Potassium hydrogen fluoride                    | 238.8              | 55.8                                 | 0.024                    | 84.8                          | n.a.                        | 2370                              | [57]    |
| Myo-inositol                                   | 224                | 126.4                                | 0.072                    | 260                           | n.a.                        | 1750                              | [57]    |

**Table 6b**

Phase change materials for triple effect absorption chiller based solar cooling systems.

| Property                      | LiOH(30)–70NaOH | NaOH(20)–80NaNO <sub>2</sub> | NaOH(73)–27NaNO <sub>2</sub> | LiNO <sub>3</sub> (45)–47NaNO <sub>3</sub> –8Sr(NO <sub>3</sub> ) <sub>2</sub> | LiNO <sub>3</sub> (87)–13NaCl | KNO <sub>3</sub> (54)–46NaNO <sub>3</sub> | NaNO <sub>3</sub> (54)–46KNO <sub>3</sub> |
|-------------------------------|-----------------|------------------------------|------------------------------|--|-------------------------------|---|---|
| Melting point (°C)            | 210–216         | 230–232                      | 237–238                      | 200  | 208                           | 222                                       | 222                                       |
| Latent heat of fusion (kJ/kg) | 278–290         | 206–252                      | 249–295                      | 199  | 369                           | 100                                       | 117                                       |
| Ref.                          | [60]            | [60]                         | [60]                         | [60]   | [60]                          | [60]                                      | [60]                                      |

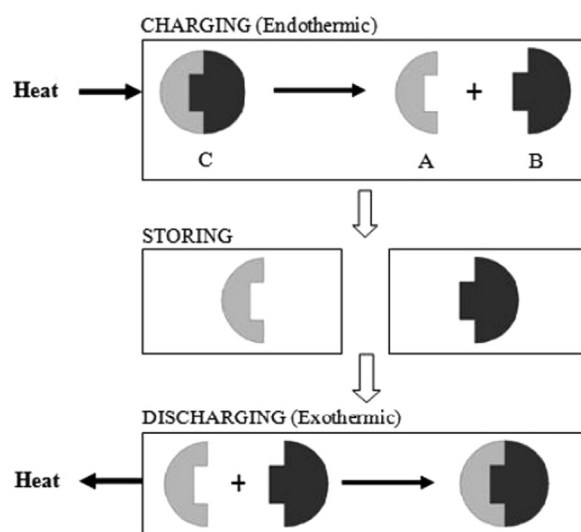
#### 4.2.3. PCMs for solar cooling applications

Table 4 presents materials, and their relevant properties, with possible application in single-effect absorption & desiccant cooling systems (phase change temperature around 60–100 °C) [8,53–56]. For practical reasons and in order to avoid redundancies with the previous literature the authors decided to not report all the available materials. Since their properties are not competitive with water (e.g. the benefits of the higher energy density is not sufficient to cover the extra investment cost), only few of them along with their complete set of properties have been reported. Table 4 is a snapshot of the PCMs candidates available in that temperature range.

Table 5 summarizes the materials with possible application in a double-effect absorption system (phase change temperature around 140–190 °C) [53,55]. Data on thermal conductivity and specific heat capacity have not been found.

Except for a few metal alloys [51], literature on PCMs suitable for triple effect chillers does not exist. Hence, databases such as CRC handbook [57] have been used to identify potential candidates. These materials were chosen (Table 6) to have melting point between 200–240 °C, relatively high heat of fusion and safety requirements (according to MSDS [58]) suitable for a rooftop application (e.g. high flashing point). Information on the cost of these materials has not been obtained at this stage.

Down-selection of suitable materials from the above list is complicated by competing properties exhibited by these candidate materials. For example, metals (Table 6a) identified for high temperature application have high thermal conductivity and energy density. However, their cost indices are orders of magnitude higher than salts (90 times higher [61]). Salts due to their low thermal conductivity often need mechanisms to enhance thermal conductivity that could result in a complex system design. Lack of sufficient information (thermo physical, cost data as noted in the above tables) and performance testing results also hinders their

**Fig. 7.** CHTES mechanism [62].

easy down-selection for novel applications. For example, materials with good thermal properties have been listed in these tables (e.g. D-mannitol, Galacticol, KCl+ZnCl<sub>2</sub>, Metaboric acid). However, detailed economic analysis and long term performance tests are needed before they can be treated as potential candidates along with water for high temperature applications.

#### 4.3. Thermo-chemical Materials

Thermo Chemical Thermal Energy Storage (CHTES) materials rely on the energy absorbed and released in breaking and reforming molecular bonds in a completely reversible chemical reaction.

Fig. 7 depicts the storage mechanism of thermo chemical materials.

Thermo-chemical thermal energy storage materials have the highest energy density among other technologies [63]. These materials also have a big advantage of very small losses because energy can be stored as reactants at ambient temperature. Instead, physical thermal storage (sensible, latent) materials have thermal losses through heat conduction, convection and radiation. General characteristics of CHTES are summarized in Table 7.

Thermal energy storage through sorption phenomena are also normally considered as thermo-chemical storage [64]. In sorption systems, heat is needed to overcome the bonding between working fluid molecules and the sorption material molecules. As a result, the sorption material is dried. When the working fluid molecule is adsorbed on the sorption material, heat is released. Sorption systems are normally investigated for their refrigeration applications. ClimateWell, a Swedish solar cooling system supplier has demonstrated a Lithium Chloride (LiCl) salt based thermal storage system [65].

CHTES materials are predominantly in research and development phase. However possible chemical reactions suitable for solar cooling applications are listed in Table 8.

## 5. Thermal storage system design

The Thermal Energy Storage System (TESS) does the function of (i) containing the storage media, and (ii) providing a means to transfer heat to and from the media (either through heat transfer

equipment or directly). Ideally, it will segregate heat such that heat transfer fluid is directed to the thermally driven cooling device at the highest possible temperature and heat transfer fluid is delivered to the solar collector at the lowest possible temperature, while maximizing energy stored at useful temperature.

For a practical TESS design, details of the storage material (discussed in the previous section) and the operational constraints of other components of the plant (e.g. solar collector, chiller) are required.

Thermal energy storage systems are classified as active and passive systems according to the way heat is transferred to the storage media (Fig. 8).

Some literature on thermal energy storage for solar power plants, suggests that active systems are defined as using a fluid as the storage medium which is circulated through a heat exchanger(s) (through the collector loop and/or through the power generation loop). Passive systems use a solid storage medium and the heat transfer fluid passes through the storage medium only for charging and discharging [11,68].

This definition can be confusing for researchers dealing with active and passive systems in the context of Domestic Solar Hot Water (DSHW) systems. In active DSHW systems, heat is delivered to the storage tank from the collector by means of a circulation pump whereas in a passive DSHW system, the heat is transferred through natural convection means. Fig. 9 shows a schematic of an active and passive DSHW system.

As discussed in section two, hot water based storage systems predominate in solar cooling systems. Hence, the definition of active and passive systems in the context of DSHW systems will be used in this article. Due to the limited applicability of passive systems (systems that operate without a pump) in large scale solar cooling installations, passive thermal energy storage systems are not discussed further in this article.

Active thermal storage systems are normally sub divided into direct and indirect systems. In direct systems, a single heat transfer fluid is used for (i) transferring heat from the solar collector to the thermal store, (ii) transferring heat from the thermal store to the thermal cooling device and (iii) storing the heat as the heat storage medium. Alternatively, in indirect

**Table 7**  
General characteristics of CHTES materials experimentally tested.

| Performance parameter | CHTES (sorption and thermo-chemical)  | Ref.    |
|-----------------------|---|---------|
| Temperature range     | 20 to > 2500 °C   | [11,62] |
| Storage density       | Normally higher than STES and LHTES: 0.5 to 5 GJ/m <sup>3</sup>   | [11,62] |
| Lifetime              | Depends on reactant degradation and side degradation  | [62]    |
| Technology status     | Generally not available, but undergoing research and pilot project tests  | [62]    |
| Advantages            | High storage density<br>Low heat losses (storage at ambient temperatures)<br>Long storage period suitable<br>Long distance transport possibility<br>Highly compact energy storage | [62]    |
| Disadvantages         | High capital costs<br>Technically complex   | [62]    |

**Table 8**  
Thermo-chemical material for solar cooling applications.

| Thermo-chemical material          | Charging temperature (°C) | Reaction  | Energy density (kWh/m <sup>3</sup> ) | Ref.    |
|-----------------------------------|---------------------------|---|--------------------------------------|---------|
| Strontium bromide exahydrate      | 70–80                     | $\text{SrBr}_2 \cdot 6\text{H}_2\text{O} \leftrightarrow \text{SrBr}_2 \cdot \text{H}_2\text{O} + 5\text{H}_2\text{O}$                              | 60                                   | [48]    |
| Sodium sulfide pentahydrate       | 83                        | $\text{Na}_2\text{S} \cdot 5\text{H}_2\text{O} \leftrightarrow \text{Na}_2\text{S} \cdot 2\text{H}_2\text{O} + 3\text{H}_2\text{O}$                 | 510–780                              | [48]    |
| Calcium chloride dihydrate        | 95                        | $\text{CaCl}_2 \cdot 2\text{H}_2\text{O} \leftrightarrow \text{CaCl}_2 \cdot \text{H}_2\text{O} + \text{H}_2\text{O}$                               | 200                                  | [48]    |
| Magnesium sulphate heptahydrate   | 122–150                   | $\text{MgSO}_4 \cdot 7\text{H}_2\text{O} \leftrightarrow \text{MgSO}_4 + 7\text{H}_2\text{O}$   | 420                                  | [48]    |
| Magnesium chloride exahydrate     | 150                       | $\text{MgCl}_2 \cdot 6\text{H}_2\text{O} \leftrightarrow \text{MgCl}_2 \cdot 2\text{H}_2\text{O} + 4\text{H}_2\text{O}$                             | 589                                  | [66]    |
| Magnesium sulphate heptahydrate   | 150                       | $\text{MgSO}_4 \cdot 7\text{H}_2\text{O} \leftrightarrow \text{MgSO}_4 \cdot \text{H}_2\text{O} + 6\text{H}_2\text{O}$                              | 686                                  | [66]    |
| Magnesium chloride exahydrate     | 150                       | $\text{MgCl}_2 \cdot 6\text{H}_2\text{O} \leftrightarrow \text{MgCl}_2 \cdot \text{H}_2\text{O} + 5\text{H}_2\text{O}$                              | n.a.                                 | [48]    |
| Calcium chloride dihydrate        | 150                       | $\text{CaCl}_2 \cdot 2\text{H}_2\text{O} \leftrightarrow \text{CaCl}_2 + 2\text{H}_2\text{O}$   | 400                                  | [66]    |
| Aluminum sulphate octadecahydrate | 150                       | $\text{Al}_2(\text{SO}_4)_3 \cdot 18\text{H}_2\text{O} \leftrightarrow \text{Al}_2(\text{SO}_4)_3 \cdot 5\text{H}_2\text{O} + 13\text{H}_2\text{O}$ | 600                                  | [66]    |
| Iron carbonate                    | 180                       | $\text{FeCO}_3 \leftrightarrow \text{FeO} + \text{CO}_2$  | 722                                  | [11]    |
| Copper sulphate pentahydrate      | 200                       | $\text{CuSO}_4 \cdot 5\text{H}_2\text{O} \leftrightarrow \text{CuSO}_4 \cdot \text{H}_2\text{O} + 4\text{H}_2\text{O}$                              | 574                                  | [48,67] |
| Metal hydrides                    | 200–300                   | $\text{Metal } x\text{H}_2 \leftrightarrow \text{metal } y\text{H}_2 + (x-y)\text{H}_2$   | 1111                                 | [11]    |
| Methanol                          | 200–250                   | $\text{CH}_3\text{OH} \leftrightarrow \text{CO} + 2\text{H}_2$  | n.a.                                 | [11]    |
| Magnesium oxide                   | 250–400                   | $\text{Mg}(\text{OH})_2 \leftrightarrow \text{MgO} + \text{H}_2\text{O}$  | 917                                  | [11]    |

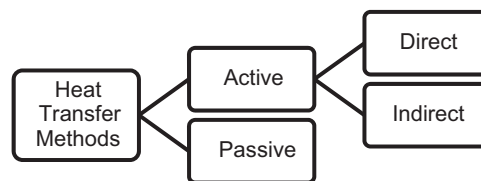


**Fig. 8.** Thermal storage system classification

systems, heat from the solar collectors is transferred into a different medium, via a heat exchanger, at some point in the process before it arrives at the thermal cooling device.

Direct storage systems have a number of distinct advantages in solar cooling applications. In addition to reducing cost, the elimination of additional heat exchangers (i) prevents the resulting degradation of temperature from the solar source to the thermal cooling device and (ii) reduces the need for additional pumped flow circuits with associated parasitic power consumption. Eliminating the degradation of temperature is particularly important for maintaining cooling capacity in the thermal cooling device during periods of reduced solar radiation.

In the following discussions, literature available on active thermal storage systems are divided into systems based on sensible storage media (water) and phase change storage media. Other active storage systems, used in solar power generation applications, are briefly reported in order to widen the potential options available to the solar cooling designer utilizing experiences gained from related solar thermal applications.

### 5.1. Active TESS using water as storage media

Where frosting is not an issue, water can be pumped directly into the thermal store from the solar collectors. In this way solar heated hot water enters the top of the storage tank and cooler water is withdrawn from the bottom of the tank to go to the solar collectors. If sufficient temperature rise is achieved over the collector, then thermal stratification can be achieved in the storage tank, being a distinct temperature separation between hot water

at the top of the tank and cooler water at the bottom of the tank. Conversely, if the temperature rise over the solar collectors is low, or if the mixing effect of water flowing into and out of the tank is high, then the water in the tank may rise and fall as a single block of well mixed fluid.

The thermodynamic benefits (increase in exergy and thermal performance) of stratification have been highlighted by many authors [70–72]. Thus hot water storage tank design requires careful consideration of stratification effects, management of flows and other overall solar cooling system design considerations.

Cost implications of pressurized systems (resulting from desired operation at elevated temperatures) may dictate the use of a heat exchanger interposed between the collectors and the storage tank to decouple the heat transfer fluid from the storage media. Similarly, indirect heat exchanger arrangements are often required for freezing protection [73]. A wide range of heat exchanger/storage tank configurations have been identified including location of heat exchangers inside or outside of the storage tank [74,75].

The addition of a backup heat source can also be either (i) integrated into the storage tank or (ii) located external to the storage tank in the thermal cooler supply flow loop. Some configurations are illustrated in Fig. 10. The typical design return temperature from the generator of a thermal cooling device is around 5 to 10 °C lower than the inlet temperature. This low temperature difference between the supply and return hot water temperatures can influence the ability to achieve thermal stratification in the thermal store, and can potentially lead to heat from the backup heater warming the hot water tank and thus reducing

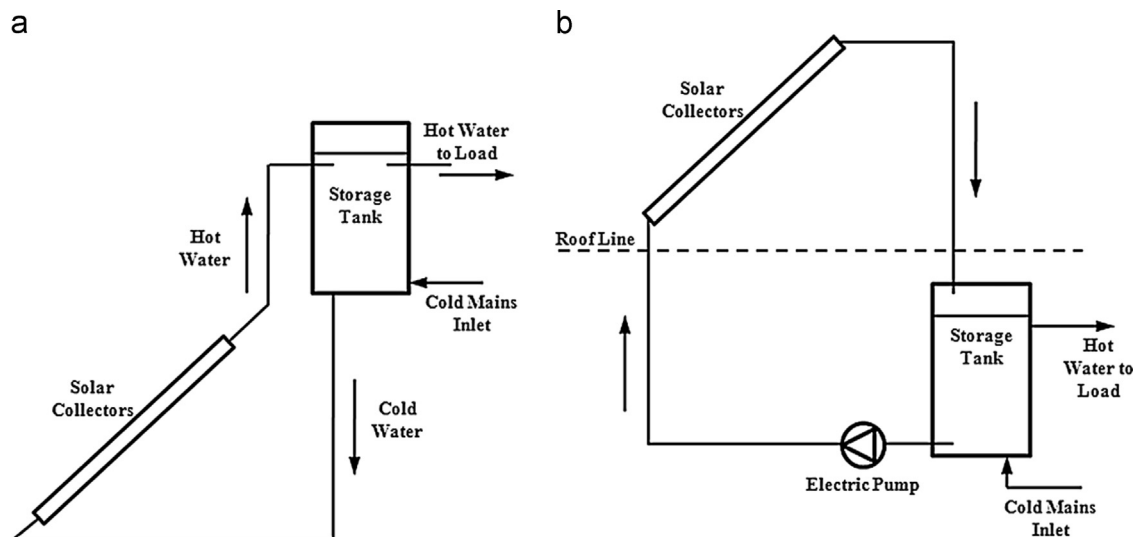


Fig. 9. Difference between a solar domestic hot water (a) passive and (b) active system [69].

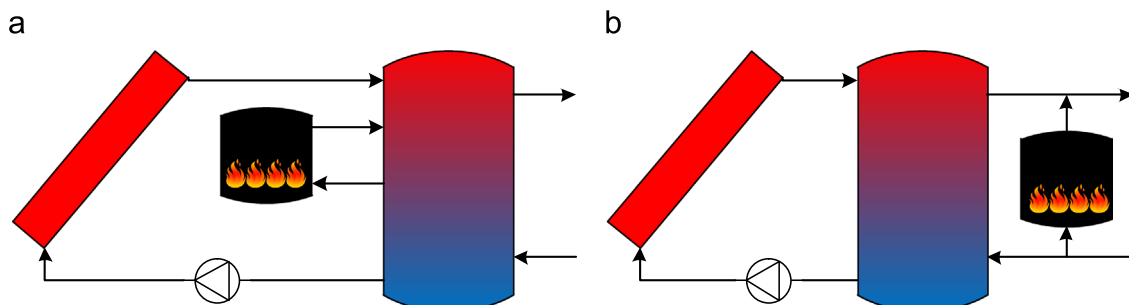


Fig. 10. Two possible configurations of the back-up heat source: integration in the tank (a) and external in parallel with the tank (b), adapted from [23,76].

the efficiency of the solar collector. Mounting a backup heater separately and in parallel to the thermal storage tank (Fig. 10(b)) is recommended.

#### 5.1.1. Stratification improvements

Ideally, the storage system should be developed to optimize thermal stratification for the considered application. In order to fulfil this task, several guidelines have been proposed in the literature. They mainly deal with optimizing the aspect ratio of the tank (tank height versus its diameter) and positioning of inlet and outlet pipes.

In their computational fluid dynamics simulations, Ievers and Lin [72] concluded that increasing the aspect ratio from 2.5 to

3 leads to a 22.6% increase in thermal stratification, whereas change in aspect ratio from 2.5 to 5 yielded 30.7% benefit. The authors recommended an ideal aspect ratio of 3.5 as a value to achieve a good level of stratification within the tank. Further they underlined that higher aspect ratio tanks have bigger heat losses due to larger heat transfer surface area. Al-Marafie et al. [77] concluded that aspect ratios bigger than 4 are not desirable because the resulting added cost does not lead to big improvement in the thermal performance. Ievers and Lin [72] also concluded that moving the position of the inlet/outlet ports towards the tank outer extremities improved the degree of stratification. They found that an offset of 150mm from the tank top/bottom reduced thermal stratification by 28% and an offset of 300 mm yielded 72% reduction in thermal stratification. Rosen et al. [71]

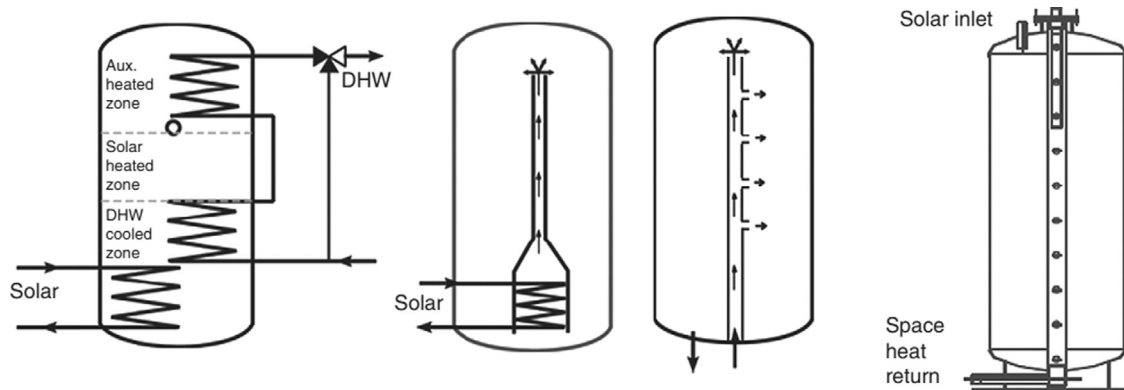


Fig. 11. Options for obtaining stratification in solar hot water tanks: (from left) several internal heat exchangers, stratifying pipe with single output (single stratifier), internal and external pipe with multiple stratifiers [78].

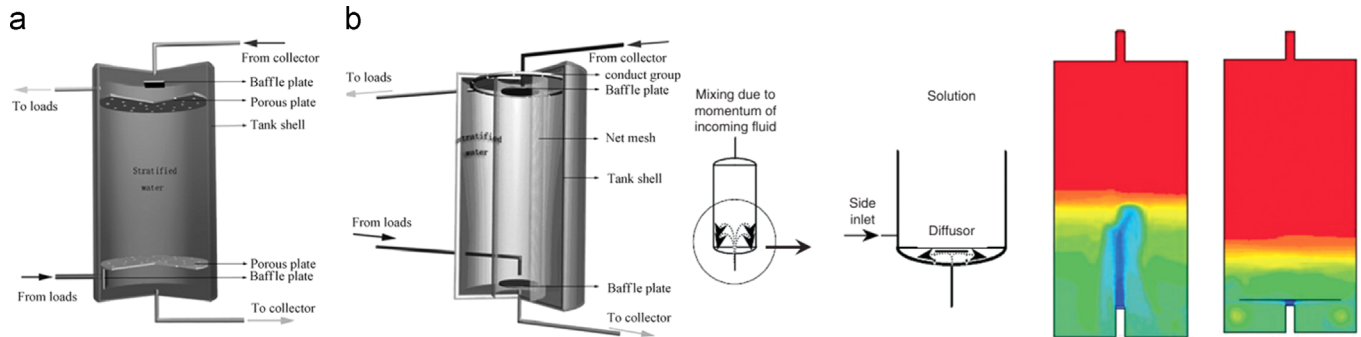


Fig. 12. Design concepts for solar hot water systems to inhibit mixing [73,76].

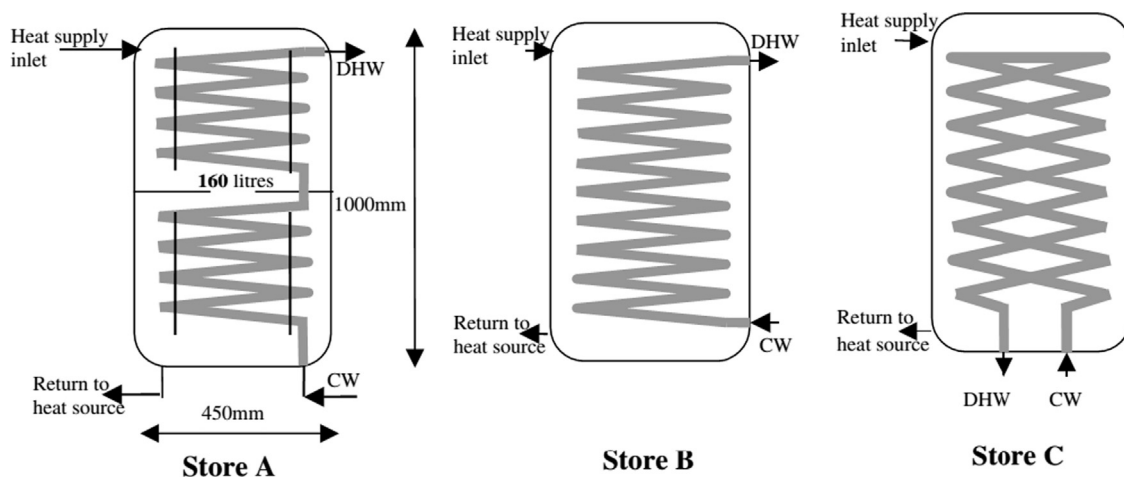


Fig. 13. Design concepts for indirect heat exchanger solar hot water systems [79].



proposed a “good design” in terms of port location: inlet/outlet at the top/bottom tank. Four different ways to achieve stratification through tank design was explored by Streicher and Bales [78] as shown in Fig. 11.

Han et al. [73] studied ways to inhibit turbulence that results in mixing of hot and cold water in these tanks. They proposed measures such as adding a baffle plate at tank inlet, adding a porous mesh to slow down water flow and adding a diffuser at the inlet to maintain stratification (Fig. 12):

In the case of indirect storage systems (systems with heat exchanger), three new design concepts were investigated by Spur et al. [79]. They concluded that type A (“bottom” and “top” coil) has the best thermal performance in order to promote the stratification (Fig. 13), given a realistic daily domestic hot water draw-off profile.

## 5.2. Latent heat applications

There are various applications of Latent Heat based active Thermal Energy Storage Systems (LHTESS) pertaining to the cold side of the cooling device [54,80–82] including;

- Ice storage; and
- Thermal storage in the fabric of an air-conditioned building (e.g. PCM layer in the floor).

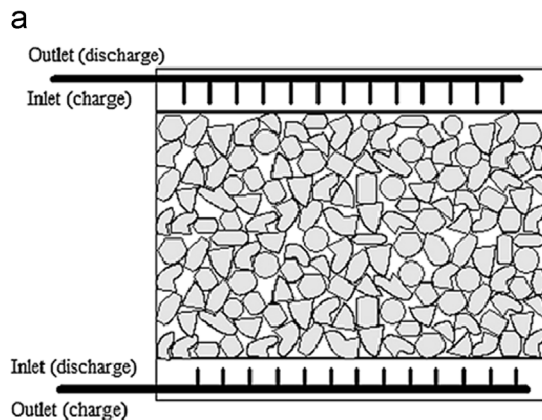
Since this article focuses on storage of heat from solar collectors in the range 60 to 250 °C, cold storage is not exhaustively discussed in this article, but only few examples are reported. It may be noted here that these heat transfer approaches are still relevant for high temperature latent heat storage for solar cooling applications.

According to Mehling et al. [54], heat transfer with PCMs can be divided into three types: exchanging heat at the outer surface of the thermal store [83–85], exchanging heat on large surfaces within the thermal store [86–88], and exchanging heat by exchanging the storage medium itself (mainly PCM slurries).

Regarding the second type, two heat transfer design concepts for LHTESS are widely found in the literature. They are:

- a. Packed bed storage
- b. Shell and tube/compact heat exchanger storage

Packed bed storage systems consist of a storage tank filled with solid capsules or solid material. The heat transfer fluid passes through this bed. The solid materials fill the storage container as shown in Fig. 14a.



The shell and tube LHTES with PCM was heavily investigated from the late 1970s until the 1990s [89–94]. According to Longeon et al. [95] the shell and tube is the most promising technology with LHTES since it lowers the system cost. The concept consists of a series of tubes grouped in a bundle and embedded in a mantle or shell, as shown in Fig. 14(b). Some researchers investigated the configuration with the PCM filling the annular space between the outer tube surface and the shell, others the encapsulation of the PCM within the pipe. Jegadheeswaran and Pohekar [96] have summarized studies on finned tubes in LHTES with PCM.

Table 9 summarizes the literature on packed bed and shell-and-tube heat storage systems. More information about packed bed latent heat thermal energy storage with PCMs capsules can be found in the review by Regin et al. [97].

More recently, Oró et al. [98] have focused on the development of a LHTES based on a shell and tube design for solar cooling applications involving double effect chillers (140–200 °C). The experiments with hydroquinone as storage media were performed for two different designs: finned and un-finned shell-and-tube TES [38]. The aim of the work was to experimentally test and compare the average effectiveness of the two TES systems. For the un-finned configuration, the authors concluded that the average efficiency curve, calculated with empirical models published in the literature, fits the results well even when the tank and tube dimensions are changed. For the finned unit, the effectiveness curves did not match.

The empirically derived equation used to calculate the effectiveness is

$$\bar{\epsilon} = \frac{Q_{\text{experiment}}}{Q_{\text{theoric}}} = \frac{\bar{T}_{HTF,in} - \bar{T}_{HTF,out}}{\bar{T}_{HTF,in} - T_{PCM}} = 1 - \exp[-0.0199(\dot{m}/A)] \quad (4)$$

Where  $T_{HTF}$  is the average HTF temperature for the inlet and outlet port, while  $T_{PCM}$  is the average phase change temperature of the PCM,  $\dot{m}$  is the mass flow rate of the HTF through the thermal store and  $A$  the heat transfer surface area. The effectiveness is described as a ratio of the actual heat (dis)charged over the theoretical maximum heat that can be (dis)charged. This correlation is valid for similar configurations of the storage and HTF conditions.

## 5.3. High temperature solar thermal applications

A range of additional TESS designs have been proposed for solar power generation applications which could also be applicable for high temperature (e.g. double and triple effect absorption chiller) solar cooling applications. There are many reviews on such technologies [11,44,68,114–119]. A summary of these systems that could be applied to solar cooling are presented in Table 10.



Fig. 14. Two LHTESS concepts: packed bed (a) and shell-and-tube (b) heat storage designs [37,69].



**Table 9**

Summary on the studies on packed bed (PB) and shell-and-tube (S&amp;T) heat storage systems.

| Type | Study   | PCM                            | HTF  | Activity/Conclusions/Results   | Ref.  |
|------|---|--------------------------------|--|--|-------|
| PB   | Test of three configurations of storage units with PCMs   | Various                        | Air  | PB performed better than the LHTES units with horizontal or vertical encapsulated PCM cylinders in terms of heat transfer rate   | [99]  |
| PB   | Testing thermal energy storage for air conditioning/refrigeration   | n.a.                           | Anti-freeze solution   | Simulation of the (dis)charging process taking into consideration the heat transfer within the PCM packing system and with the surrounding heat transfer fluid   | [100] |
| PB   | Experimental investigation on combined sensible and latent PB   | Paraffin ( $T_m$ 60 °C)        | Water  | Results showed that combined unit gave better performance if there was direct mixing of HTF with tank hot water  | [81]  |
| PB   | Investigation on the dynamic performance of solar heat storage system using packed bed  | Myristic acid                  | Water  | Influences of HTF inlet temperature and flow rate, initial temperatures of HTF and PCM on the latent efficiency and heat release rate were analyzed  | [101] |
| PB   | Study on the effect of different capsule sizes and materials as well as the effect of varying the HTF flow rate and inlet temperature | Water/Ice                      | Water + 35 wt% Ethylene glycol                                   | EER (defined as the ratio of the average energy regained rate to the average energy stored rate under the same operational conditions) is better with metallic capsules  | [102] |
| PB   | New PB concept design   | n.a.                           | n.a.   | Application of spherical capsules of different sizes in order to best match the required temperature profile (stratification) along the storage tank   | [103] |
| S&T  | Experimental and numerical investigation of finned S&T HEX  | Water/Ice                      | Ethyl-alcohol  | Numerical simulations to investigate the effect of fin and flow parameters on energy storage and amount of solidification. Comparison with experimental results.   | [104] |
| S&T  | Novel shell-in-tube TES: shell inclined in order to assist with natural convection  | Paraffin                       | Water  | Three types of paraffin tested. The configuration was found to be very useful since the heat transfer improved   | [105] |
| S&T  | Study of performance of cold storage during the solidification process (discharge)  | Unknown PCM $T_m$ 8 °C         | n.a.   | The foils were found to be an efficient way for enhancing the heat transfer because foil has high heat conductivity  | [106] |
| S&T  | Optimization of a LHTES with embedded heat-pipes  | KNO <sub>3</sub>               | Therminol  | Development of a thermal resistance network model of a shell-and-tube tank with embedded heat pipes. The study serves as guideline for design a LHTES.   | [107] |
| S&T  | Experiments on charging and discharging periods on LHTES  | Water/Ice                      | n.a.   | The experimental data indicated that after short heat conduction dominated period, the heat transfer was mainly driven by natural convection. For charging, the tube thermal conductivity, HTF inlet temperature and shell diameter had a strong influence on the storage heat capacity; for discharge, the most important parameter was the HTF inlet temperature | [108] |
| S&T  | Investigation of the performance enhancement of a S&T with dispersion of high conductivity nano-particles                             | Paraffin wax and hydrated salt | Water  | Comparison of two enhanced PCMs (org. and inorg.) based on charging/discharging modes, exergy stored/recovered and exergy efficiency. The hydrated salt (inorg.) composites showed better exergy efficiency than paraffin wax (org.) due to their higher thermal conductivity, although the former stored/recovered less exergy than the other.                    | [109] |
| S&T  | Study on integral heat pipes for concentrating solar power (CSP)  | KNO <sub>3</sub>               | Therminol  | An approach to reduce the thermal resistance of PCM has been investigated: immersion of the heat pipes into the PCM matrix in different configurations. Higher effectiveness was obtained with the four tubes configuration for both the modules.  | [110] |
| S&T  | Experimental investigation of the dynamic melting in a LHTES  | Water and hydrated salt        | non-combustible, aqueous based fluid with dissolved ionic solids | The approach to enhance the heat transfer involved recirculation of the melted PCM. The technique had higher effectiveness and shorter melting times, further the effective PCM thermal conductivity doubled without a reduction in the compactness factor   | [111] |
| S&T  | Experiments on horizontal S&T LHTES   | Paraffin                       | Distilled water  | The melting behavior dramatically changed between the bottom and top part of the storage unit.   | [112] |
| S&T  | Modeling of a S&T LHTES   | Erythritol                     | Dow Corning 550 oil  | Simulations of different pipes configurations. The simplified 3D approach predicted heat transfer rates to within 8.5% compared to the 2D detailed model.  | [113] |

**Table 10**

Examples of high temperature thermal energy storage systems used in solar power generation plants.

| Type                | TES system                         | Storage media                           | Characteristics of the system  | Ref.         |
|---------------------|------------------------------------|---|--|--------------|
| Direct/<br>indirect | Steam accumulator and its variants | Steam/water                             | <ul style="list-style-type: none"> <li>• Short reaction times</li> <li>• High discharge rates</li> <li>• Low thermal capacity</li> </ul>   | [120]        |
| Direct/<br>indirect | Two-tank storage                   | Salt (e.g. solar salt)                  | <ul style="list-style-type: none"> <li>• Higher system theoretical thermodynamic efficiency</li> <li>• Cost reduction of the tank: the cold one suffers less thermal stress</li> </ul> | [121–124]    |
| Direct/<br>indirect | One-tank thermocline storage       | Oil, molten salt                        | <ul style="list-style-type: none"> <li>• Cost reduction in comparison of the two-tank system</li> </ul>  | [44]         |
| Indirect            | Solid thermal energy storage       | Concrete, castable ceramic, sand, rocks | <ul style="list-style-type: none"> <li>• Cost reduction due to non pressurized tank</li> <li>• Mostly low cost materials</li> </ul>  | [43,119,125] |

## 6. Control approaches for solar cooling systems

So far we have focused mainly on the solar cooling system configuration, storage materials and thermal storage equipment involved in the design of an effective solar air conditioning plant, but with limited focus on its continuous operation over the wide range of conditions that could be encountered throughout a year. Specifically a practical operating system will need a set of control strategies to manage charging and discharging of the thermal store in a manner that is robust and efficient under all conditions. From a control perspective, this is not straightforward because the thermal energy store is highly integrated with other parts of the system such as the solar loop, the absorption chiller and any backup heat source. Importantly it is well known that the control system has a massive impact on system efficiency [126].

Control of a solar air-conditioning (AC) plant involves management of both continuous states (e.g. temperatures, speeds of variable-speed pumps, position of three-way mixing valves) and discrete states (e.g. open–close valves, on–off state of backup boilers, on–off state of pumps) subject to variations in cooling demand and solar irradiation (the main source of energy) that cannot be manipulated and may fluctuate significantly. Inherent time delays are present due to fluid transportation, and the process dynamics vary with the environmental conditions [127].

It is claimed that the solar and storage loops of a solar system are the most challenging to control because they are the most affected by the transient nature of solar irradiation [128]. The main objective of the controller is to equalize, totally or partially, this transient effect.

Three control strategies are presented by Kohlenbach [128] for charging the thermal store via the solar collector flow loop:

- (1) Differential on–off: A constant flow pump is switched on or off based on the temperature difference between the fluid in the collector and the thermal store. This approach is simple and common but presents large fluctuations in collector outlet temperature and, because of its on–off nature, can result in higher collector thermal losses and lower solar gains.
- (2) Temperature difference based: A proportional (P) controller is used to drive a variable-speed pump based on the temperature difference between the solar collector and the thermal store. Besides smaller temperature oscillations, thermal losses are reduced due to less standstill time while operating.
- (3) Radiation based: Again a proportional controller is used to drive the pumps speeds, but based on measurement of relative changes in solar radiation (e.g. with a PV cell). For each solar AC system, a different empirical correlation between radiation and pump speed is necessary. This controller can achieve almost constant values in collector outlet temperatures.

The first two control schemes are used in small domestic systems, while the radiation-based strategy is mainly used for large systems, where very stable output temperatures are worth the extra hardware cost of the radiation sensor. The second and third schemes should be applied in the case of a LHTESS, in order to match the collector outlet temperature with the phase change temperature. Simulations showed a 6% improvement in yield factor when the third control strategy was compared with the first and second (which had similar performance). However, when applied in a real system, similar performance across all three techniques was observed, and thus it was concluded that the simplest control technique (differential on–off) was as good as the others in terms of yield factor for that particular plant [128].

From a whole-system point of view, Bujedo et al. [129] have studied three different control strategies applied to a real-world

solar AC plant operating over three years, with both hot and cold storage. These strategies are as follows:

- Strategy 1 (business as usual): The mass flow of hot water going into the chiller is fixed and the load control is done by cycling the chiller on and off. The pumps in the solar collector switch on anytime the radiation exceeds a threshold ( $300 \text{ W/m}^2$ ). Solar-heated water is delivered to the chiller (i.e. the backup boiler is turned off) any time the temperature of the highest part of the tank is higher than that of the generator outlet of the chiller.
- Strategy 2: consists of varying the temperature of the condenser inlet in the chiller as a function of the generator temperature to maintain maximum COP. Variable-speed pumps in the solar collector switch on based on “critical radiation”, which is the minimum radiation necessary for the tanks to reach a given set-point temperature [130]. This strategy optimizes the use of available radiation and uses less electricity by running collector pumps only at necessary speed. The chiller is still cycled.
- Strategy 3: the goal is to maintain the temperature at the bottom of the cold storage at a constant  $10^\circ\text{C}$ . Similar to strategy 2, the temperature of the condenser is varied but also the generator mass flow is adjusted as a function of the system load. Thus, the chiller works without interruptions, resulting in higher COP because there is no cycling.

Experimental results indicate that strategy 3 outperforms both strategies 1 and 2: for example, it achieved 12.61% more solar field efficiency and almost tripled the solar fraction of strategy 1.

With the exception of the approach described above, most of the literature on control of solar air conditioners involves alternative hardware designs that require new controllers to operate the modified system. Thus, rather than answering the question of how to operate an existing system more efficiently, these approaches focus on how to obtain maximum benefit from new equipment. For example, Rosiek & Batlles [131] aimed to reduce the energy consumption of a solar-assisted air conditioning system for a research center consisting of offices and labs by incorporating chilled water storage and occupancy sensors. Their main control variables were whether or not each of the 16 fan-coil units was operating (based on the occupancy sensors) and where the chilled water comes from (cold storage or absorption chiller, and in the case of the latter, whether or not it is necessary to switch on the backup heater). The modified system used 42% less energy than the original configuration.

Another example of a modified system is reported by Li & Sumathy [132], where the hot storage tank is divided in two partitions, the upper one having one quarter of the volume of the whole tank. The controller decides whether to operate the system using the whole tank or just the upper partition. This decision is made depending on the temperature of the stored hot water, and whether or not the useful solar energy gain is larger than the cooling load. By using the partition early in the day and switching to full tank, as enough solar energy becomes available, the authors report that solar cooling can be started 2 h earlier and that the COP of the whole system increases by 15%.

### 6.1. Advanced model-based and look-ahead control approaches

None of the approaches discussed so far take into account future (look-ahead) events such as weather and building occupation predictions. The appeal of look-ahead controllers which optimize the values of interest (e.g., temperature in air conditioned spaces and energy cost) using a model of the system and several forecasts (weather, occupancy, electricity price), is that these controllers can

plan for the future by considering alternatives beyond the scope of the above “Model-free” controllers. For example, based on the weather and occupation forecast for the following day, a look-ahead controller might decide to charge the thermal store only partially the day before. The use of such predictive controls could provide additional potential for better matching of the intermittent solar resource with the varying demand for cooling, resulting in increased solar fraction and reduced backup energy consumption.

Developing mathematical models is a key element of a look-ahead controller, as a model allows simulation of what the system would do under the forecast conditions. This enables planning of the best control strategy for these conditions. For example, Pasamontes et al. [133] identified a model for a solar hot water system using first-principle equations and used artificial intelligence methods to identify the best values for unknown system parameters. Models like these can then be used to develop look-ahead controllers, such as the well known [134] “Model Predictive Control” (MPC).

Charging the thermal store based on forecast temperature and solar irradiance is presented by Mammoli et al. [135], who optimized the operation of a solar-assisted HVAC system with both hot and cold thermal storage. In their control strategy, the hot thermal store is charged using solar collectors and used to run an absorption chiller, whereas the cold store is charged (normally overnight) using an electric chiller. The optimization aims to minimize energy costs by selecting (a) when during the day the absorption chiller is run and (b) how much cold storage is needed for the following day. Using temperature and irradiance forecasts, the authors estimate available cooling power from the absorption chiller, informing the decision about how much cold storage needs to be charged using the electric chiller (which gives the value for control signal (b)). They demonstrate scheduling of the absorption chiller using these forecasts, reporting 29% annual energy savings when this look-ahead scheduling is compared to the regular one, which consists of fully charging the cold storage every night and running the absorption chiller whenever there is sufficient energy in the hot storage “to allow ‘ride through’ of intermittent cloud cover”. The system is modeled and optimized using Lawrence Berkeley National Laboratory (LBNL)’s Distributed Resources Customer Adoption Model (DER-CAM).

A promising technique for look-ahead scheduling is the well-known [134] control framework called model predictive control (MPC). In MPC, a model of the system is used to simulate the effect of different possible control sequences and an optimization problem is solved for a certain time horizon to seek the best control sequence for a given set of objectives (e.g., maintain a given temperature and reduce energy consumption). MPC takes into account the fact that neither models nor forecasts are perfect by only implementing on the plant the very first time step of the control sequence obtained via simulation. Iteratively, when feedback information about the actual state of the system arrives, the optimization problem is solved again, and the control signal corresponding to a new time step is implemented.

Applying MPC to hybrid systems, such as a solar cooling plant, results in an optimization problem with both real and integer decision variables and a set of constraints. These problems are known as Mixed Integer Problems, and in general belong to the NP-category, which has the practical implication of being computationally expensive to solve. Therefore, several approaches to solar-cooling control try to reduce the complexity of this problem by either mapping a continuous variable to several values for the discrete ones [136] or by a multi-layer control approach [127,137,138].

In these studies ([127,136–138]) a solar AC plant is controlled to maintain a reference chilled water temperature while using the least amount of gas in the boilers (i.e., maximize use of solar energy). The decision variables are the speed of the pump circulating water through the solar collectors and the aperture of the three-way valve that determines how much hot water comes from the gas heater and how much from solar. Additionally, several other valves can be controlled to determine the *operational mode*: recirculation of water in the panels, charging the thermal store with solar, charging the thermal store using the gas boiler, etc.

Rodríguez et al. [136] used an artificial continuous control variable and developed a set of rules to map it to operating modes and values for the other continuous variables of the system. This way, the authors turned a mixed-integer linear programming problem into a non-linear programming one, with much faster computational times. As expected, the mapping between the artificial and real control variables is not straightforward and may result in suboptimal

**Table 11**  
Summary of control approaches.

| Main controlled variables  | Additional hardware | Model based     | Improvements   | Forecasts used                           | Ref.             |
|--|---------------------|-----------------|--|--|------------------|
| Solar loop pump speed  | Yes                 | No              | 6% more yield factor in simulations, no improvement in real-world trial        | None                                     | [128]            |
| Partitioned/whole tank operation mode  | Yes                 | No              | 2 h more solar cooling per day. 15% improvement in COP of the whole system.    | None                                     | [132]            |
| <ul style="list-style-type: none"> <li>Absorption chiller vs cold storage operation.</li> <li>ON/OFF state of individual fan-coils</li> <li>Backup heater operation</li> <li>Flow rate in collector</li> <li>Chiller on-off</li> </ul> | Yes                 | No              | 42% energy savings during summer   | None                                     | [131]            |
| <ul style="list-style-type: none"> <li>Flow rate in collector</li> <li>Flow rate into chiller generator</li> </ul>   | No                  | No              | 7.62% increase in solar field efficiency and 44% increase in total efficiency. | None                                     | [129] Strategy 2 |
| <ul style="list-style-type: none"> <li>Absorption chiller vs cold storage vs mechanical chiller operation schedule</li> <li>Cold storage SoC</li> </ul>  | No                  | Yes             | 29% energy savings   | Ambient temperature and solar irradiance | [135]            |
| Operation mode (discrete) and values of valves/pumps within modes (continuous)   | No                  | Yes             | n.a.   | None                                     | [136]            |
| Operation mode (discrete) and values of valves/pumps within modes (continuous)   | No                  | Yes             | n.a.   | None                                     | [137]            |
| Operation mode (discrete) and values of valves/pumps within modes (continuous)   | No                  | Yes             | n.a.   | None                                     | [127]            |
| Operation mode (discrete) and values of valves/pumps within modes (continuous)   | No                  | Yes (partially) | n.a.   | None                                     | [138]            |

strategies. Additionally, because the optimization problem is inherently multi-objective (maintaining the chilled water temperature while reducing the amount of gas used), they combined these objectives into a single one with a weighted sum. Although a common practice, this poses the hard question of how to choose the right weights. Lastly, these authors used a 15-minute prediction horizon so, even though their approach is look-ahead, it involves a short horizon and thus they need no forecasts.

The same plant has been controlled in [137] using a hierarchical controller. Hierarchical control is a well known and suitable candidate control strategy for interconnected systems such as a solar air conditioning plant, which considers different control levels. In [137], the authors considered a *configuration* level and a *regulatory* level. The configuration level selects the operating mode for the system by minimizing a linear function with variable weights which depend on the state of the plant and weather conditions (i.e. solar radiation). Once the operating mode is selected, the regulatory level is in charge of adjusting the variables within the mode using MPC. While the authors do not report benefits compared to normal operation, they do claim that the temperature level was maintained despite adverse weather conditions. A similar hierarchical approach is presented by Menchinelli & Bemporad [138] indicating that this type of controller is a natural candidate for solar cooling plants. Sonntag et al. [127] designed a supervisory control scheme for the same plant (used in [136–138]). Rather than using a model of the system, they used insight from experiments on the real plant as well as results from a simplified model (which they claim is inadequate to be used for control) to design a set of rules that define the operation mode and the values of the continuous variables that minimize energy consumption. The benefits of this control scheme are not quantified beyond mentioning that the controller is able to maintain the temperature at the desired level.

As seen, it is common to try and reduce the complexity of the mixed-integer problem. However, there are best-effort tools to address these problems in reasonable amounts of time without previous simplifications, such as the branch and bound method and heuristic techniques like genetic algorithms and ant colony optimization. Menchinelli & Bemporad [138] claimed to have tried this approach without success, due to inadmissibly long execution times which is important in real time control.

## 6.2. Summary

Table 11 summarizes the control approaches for a solar air conditioning plant discussed in this section. We have found that there is an increasing interest in model-based controllers and in day-ahead control scheduling incorporating forecasts which as discussed offer the potential for increased solar utilization and increased efficiency.

## 7. Design process approaches for thermal storage system selection for solar cooling

Design of the solar cooling TESS is integrated with the design of complete system. Design steps can be broken down as follows:

- *Step 1:* Qualitative selection of key components and storage strategy. This step is discussed in Sections 2,3 and 4 and leads to the selection of the storage material and the heat exchange configuration that is relevant to the intended solar cooling flow-sheet concept.
- *Step 2:* Quantitative assessment of storage capacity. This step is discussed in this section and is dependent on information from the other steps.

**Table 12**  
Examples of TESS optimization for solar thermally activated system.

| TESS type | Optimization tool/method  | Optimization objectives   | Optimization parameters  | Results/Conclusions   | Ref.  |
|-----------|---|---|--|---|-------|
| Sensible  | Artificial neural network (ANN), Genetic algorithm (GA)                               | Life-cycle savings (LCS)  | Collector area, storage tank volume  | The optimum solution, computed via GA, increased the LCS by 3–5% compared to the conventional “trial-and-error” method solution. The method greatly reduces the design times.                       | [142] |
| Sensible  | Parametric analysis via TRNSYS, ESS   | Solar fraction (SF), useful heat gain and auxiliary heat  | Collector area and slope, tank volume, hot water flow rate                             | The optimal parameters lead to an annual SF of 42%  | [143] |
| Sensible  | Parametric analysis via TRNSYS  | SF, yearly Primary Energy Savings (PES), Gross Solar Yield  | Collector type and area, heat rejection system, storage volume, etc.                   | The considered best solutions are not clearly chiller and application independent.  | [139] |
| Sensible  | Parametric analysis via TRNSYS  | Investment, operation cost and payback time, environmental benefits   | Collector area, chiller power, tank volume, boiler power, cooling tower type and power | A scenario has been found to optimize both environmental and economical aspects. It consisted of a absorption chiller coupled with a back-up lower capacity conventional one                        | [144] |
| Sensible  | Computer Design of Experiment (DOE), TRNSYS   | Annual PES  | Collector slope, pump flows, set-point temperatures, tank volume                       | The layout that optimized the PES vs a conventional system, has found to be unsatisfactory from the economical point of view. Its profitability can be improved only by significant public funding. | [145] |
| Sensible  | Central Composite Design (CCD), Linear Regression, Multi-objective optimization model | Present Worth Cost ratio ( $R_{PWC}$ ), Life Cycle Energy Consumption ( $R_{LCE}$ ), Life Cycle Carbon Dioxide emissions ( $R_{LCCO_2}$ ) | Collector slope and area, main and hot tank volume                                     | From the Pareto optimal front, achieving a small $R_{PWC}$ implied large $R_{LCE}$ and ( $R_{LCCO_2}$ ).  | [146] |
| Latent    | Parametric analysis via TRNSYS  | Minimizing the mechanical ventilation system size   | Ventilation strategies and air flow rates, LHTES size                                  | Free cooling showed a clear benefit in reducing the dimension of the ventilation system and in providing a better thermal comfort conditions.   | [147] |
| Latent    | Numerical simulations   | Maximize the thermal storage efficiency   | PCM type and mass, HEX dimensions, collector flow rate                                 | The selection of the PCM should be done carefully in order to produce hot water in the acceptable temperature range.  | [148] |
| Latent    | modeFRONTIER (mono and multi-objective, SIMPLEX and GA)                               | Minimizing the boiler primary energy consumption  | Tank parameters (e.g. dimensions, PCM melting temperature)                             | The insertion of PCM in a SDHW tank led to no improvements or very limited impact on the saved energy.  | [149] |



**Table 13**  
Qualitative storage sizing advice for alternative solar cooling scenario applications.

| Scenario (based on (i) technology and (ii) capacity relative to building peak demand) | Collector area options   |   |
|---|--|---|
|   | High specific collector area (m <sup>2</sup> /kW chiller capacity)       | Low specific collector area (m <sup>2</sup> /kW chiller capacity) |
| Full capacity autonomous (no back-up) solar cooling system                            | Large thermal store to manage comfort and prevent on/off cycling         | Not advisable (poor comfort outcome)                              |
| Full capacity low efficiency thermal chiller (single-stage) with gas back-up          | Large thermal store to increase solar fraction/ minimize gas consumption | Not advisable (high gas cost/ high greenhouse gas emissions)      |
| Full capacity high efficiency thermal chiller (multi-stage) with gas back-up          | Not advisable (less economic)  | Small thermal store to minimize heat losses and cost              |
| Part capacity thermal chiller with full size vapor compression chiller backup         | Not advisable (less economic)  | Sufficient thermal storage to minimize on/off cycling             |

- **Step 3:** Detailed thermal store design and operational strategy. This step is discussed in Sections 5 and 6, and provides information on how the heat will be used, the quality of the heat, and the potential for heat losses.

Numerous studies have assessed the impact of storage capacity on overall solar cooling system performance (e.g. [7,139,140]). These studies have typically used a solar energy modeling package such as TRNSYS or INSEL to perform hour by hour energy supply and energy consumption calculations on each component in the desired solar cooling system. These software packages contain weather files that provide hourly values for the solar resource (radiation intensity and direction) and ambient conditions, covering a typical year for the given location. Characteristic performance parameters for each of the key components of the solar cooling system are entered into the simulation, the fluid flow connections between components are set, and a control strategy is implemented for turning valves and pumps on/off. This enables the software to perform quasi steady-state hour by hour mass and energy balances, which can be summed over a full year to determine the annual amount of solar energy collected, the amount of backup energy required and the cooling delivered.

Typical performance evaluation criteria of merit (for possible optimization) include (i) annual primary energy savings, (ii) primary energy ratio, (iii) solar fraction and (iv) cost of primary energy. These figures of merit are defined in the International Energy Agency Solar Heating and Cooling Task38 “Solar Air-conditioning and Refrigeration” Subtask A [141].

As evident from Fig. 3, simulation and other design decision processes being employed around the world, do not appear to have resulted in any consistent “Rule-of-thumb” sizing principles. This reflects the variety of applications and the variety of optimization objectives. In the previous 10 years literature, examples of thermal storage optimization can be found both for sensible and latent TESS, as show in Table 12.

Eicker and Pietruschka [7] used INSEL to perform a parametric sensitivity analysis on a solar cooling system with a single effect absorption chiller with gas back-up. They showed that storage volume has limited impact on overall system performance when collector area is small relative to chiller size. In this case, any heat collected from the solar collectors is used immediately for cooling and there is no heat left over to store. Conversely, when collector area was high, increased storage volume led to higher solar fraction.

Henning [140] used TRNSYS to perform a parametric sensitivity analysis on solar heating and cooling in a hotel, with a single effect absorption chiller backed up by a vapor compression chiller. He found that varying thermal storage size and chiller size led to

significant variations in the cost of primary energy. However, in general, the solar fraction was clustered mainly around the size of the collector area, and increasing collector area led to progressively diminishing returns in terms of increasing solar fraction.

Fully transient modeling studies, accounting for thermal mass effects in key components, have been quite limited [150]. White [13] suggests that there exists a minimum level of thermal storage which should be included to overcome thermal mass effects at start-up, in order to prevent excessive on/off cycling of the absorption chiller.

Taking account of the breadth of these studies, the authors design advice would appear to be scenario specific along the lines given in Table 13.

While the above simulation studies assume a fixed flow-sheet and storage strategy, Noro et al. [151] used TRNSYS to compare the benefits of a solar cooling system with sensible and latent TESS alternatives, and with different quantities of storage capacity. They found that low temperature (44 °C) latent storage was the preferred option due to higher heating load. In fact it performed the highest primary energy savings.

## 8. Conclusion

This article presented an overview of thermal storage materials, storage systems, control approaches and design strategies relevant for solar cooling applications (for different set of temperature ranges). A summary of the main outcomes from this literature survey are listed below.

- Several examples of operating/demonstration units of single stage absorption chiller based solar cooling systems have been reported in the literature. All of these systems use water as the storage media. A few installations of double effect absorption chillers also use water as the storage media. Use of thermal oil as storage media for double effect chiller systems, have also been reported. Other than water and synthetic oil, materials such as concrete and asphalt are seen as potential low cost sensible storage materials.
- Many potential latent heat storage materials have been listed in this article. They have been classified according to their suitability for single effect, double effect and triple effect chillers. It is seen that salts have a good cost index but have low thermal conductivity values. A few potential phase change materials have been investigated for double effect solar cooling systems including Hydroquinone and D-mannitol which have been tested in a pilot plant. Phase change based storage materials have not been investigated for triple effect chiller



based systems. Hence a generally available database of chemicals was used to identify potential candidate materials. Metals (e.g. Sn) and metal alloys (e.g. Al–Sn) show high potential due to their melting point, thermal conductivity and energy density. However, their cost indices are likely to be orders of magnitude higher than salts.

- Hot water storage tank based storage system designs have been reviewed. Some of these designs permit use of heat transfer fluid directly in the tank whereas some other designs have a heat exchanger between the solar collector and the tank. Methods to enhance & retain stratification in these tanks have been summarized. It is seen that aspect ratio, location of inlet & outlet pipes and mass flow rate are important parameters when designing stratification based storage tanks.
- Latent heat based indirect storage systems use either packed bed storage or shell and tube heat exchangers while charging and discharging the storage media. Unfortunately there is only limited design experience for latent heat stores in solar cooling applications, with the majority of literature in latent heat system designs pertain to cold storage at low temperature.
- Controlling the charging and discharging of the thermal store, during operation of a solar air conditioning plant, is challenging due to the complexity of the system and the fluctuating nature of the main energy source. Although the control problem has traditionally been dealt with independent control of flows in the collector and chiller loops, look-ahead model-based control strategies are beginning to appear in the literature. These strategies are amenable to modern control theory tools and have the potential to deliver more efficient operational schedules over longer time periods.
- Quasi steady state mass and energy balance simulation tools (e.g. TRNSYS, INSEL) have been used extensively to size the thermal store for different applications. Surprisingly, this does not appear to have resulted in consistent sizing “Rules-of-thumb”. Careful review of the literature suggests that this results from the wide range of applications being investigated and differences in optimization objectives. A qualitative guide to storage design intent is proposed for different application scenarios.

Based on this review, key gaps in the solar air-conditioning thermal storage research topic to-date (topics for further investigation) include:

- New phase change materials (at  $\sim 180$  to  $250^\circ\text{C}$ ) for reducing the size of thermal storage in high efficiency high temperature solar cooling applications. Compared with more conventional low temperature single stage chiller systems, the extra cost (compared to water) of phase change materials would be justified by the potential reduction in pressure vessel costs, code compliance and thermal losses.
- New advanced look-ahead controls which have the ability to manage the charging and discharging of the thermal store based on forecast demand from the building and forecast availability of the solar resource. These control strategies could be used to increase solar fraction, or potentially enable greater certainty of comfort outcomes in autonomous solar thermal air-conditioning applications.
- Analysis of the impact of the thermal mass and the dilution cycle of an absorption chiller, on the minimum thermal storage size required to enable robust, predominantly steady-state operation of the chiller in solar air-conditioning applications.
- Electricity system integration studies that investigate the potential of solar cooling to smooth out electricity demand with thermal storage. Such studies would identify the electricity system wide benefits of increasing storage (which may not

be immediately evident from simple stand-alone building air-conditioning studies). It would also provide insight into how the fraction of solar energy can be increased in the electricity grid, ultimately to a future zero fossil energy grid.

## Acknowledgments

This work has been carried out as a part of the “Micro Urban Solar Integrated Concentrators” project, funded by the Australian Renewable Energy Agency.

## References

- [1] SOLAIR. Survey of available technical solutions and successful running systems: cross-country analysis; 2009.
- [2] Preisler A. Appendix 1 to IEA SHC Task 38 report D-A5: list of existing small scale solar heating and cooling plants; 2009.
- [3] Mugnier D, Jakob U. Keeping cool with the sun. *Int Sustain Energy Rev* 2012;6:28–30.
- [4] Brodribb P, McCann M. Cold hard facts 2: a study of the refrigeration and air conditioning industry in Australia. Canberra; 2013.
- [5] Hadorn J. Advanced storage concepts for active solar energy. IEA SHC Task 32 2003–2007. Eurosun 2008. Lisboa, Portugal; 2007. p. 1–8.
- [6] Furbo S, Andersen E, Fan J, Chen Z, Perers B. Thermal performance of marketed SDHW systems under laboratory conditions. Eurosun 2012. Croatia; 2012.
- [7] Eicker U, Pietruschka D. Design and performance of solar powered absorption cooling systems in office buildings. *Energy Build* 2009;41:81–91.
- [8] Sharma A, Tyagi VV, Chen CR, Buddhi D. Review on thermal energy storage with phase change materials and applications. *Renew Sustain Energy Rev* 2009;13:318–45.
- [9] Chidambaram LA, Ramana AS, Kamaraj G, Velraj R. Review of solar cooling methods and thermal storage options. *Renew Sustain Energy Rev* 2011;15:3220–8.
- [10] Al-Abidi AA, Bin Mat S, Sopian K, Sulaiman MY, Lim CH, Th A. Review of thermal energy storage for air conditioning systems. *Renew Sustain Energy Rev* 2012;16:5802–19.
- [11] Cabeza LF, Sole C, Castell A, Oro E, Gil A. Review of solar thermal storage techniques and associated heat transfer technologies. *Proc IEEE* 2012;100:525–38.
- [12] White S, Goldsworthy M. Exploitation in an unfair world: finding attractive markets for solar cooling. In: Proceedings of the 5th international conference on solar Airconditioning. Bad Krozingen, Germany: OTTI; 2013.
- [13] White S. Solar cooling training course. Sydney; 2012.
- [14] Basecq V, Michaux G, Inard C, Blondeau P. Short-term storage systems of thermal energy for buildings: a review. *Adv Build Energy Res* 2013;7:66–119.
- [15] Becker BM, Helm M, Schweigler C. Collection of selected systems schemes Generic Systems, IEA SHC Task 38 Report A2; 2009.
- [16] SOLAIR. Solair consortium, Increasing the market implementation of solar air conditioning systems for small and medium applications in residential and commercial buildings; 2014.
- [17] Calise F. High temperature solar heating and cooling systems for different Mediterranean climates: Dynamic simulation and economic assessment. *Appl Therm Eng* 2012;32:108–24.
- [18] Yabase H, Makita K. Steam driven triple effect absorption solar cooling system. In: Proceedings of the international refrigeration and air conditioning conference; 2012.
- [19] Thermax. Thermax unveils a unique solar cooling system; 2014.
- [20] Sparber B.W., Napolitano A., Eckert G., Preisler A. State of the art on existing solar heating and cooling systems. IEA SHC Task 38 Subtask B report B1; 2009.
- [21] Syed A, Izquierdo M, Rodríguez P, Maidment G, Missenden J, Lecuona A, et al. A novel experimental investigation of a solar cooling system in Madrid. *Int J Refrig* 2005;28:859–71.
- [22] Zambrano D, Bordons C, Garcia-Gabin W, Camacho EF. Model development and validation of a solar cooling plant. *Int J Refrig* 2008;31:315–27.
- [23] Pongtornkulpanich A, Thepa S, Amornkitbamrung M, Butcher C. Experience with fully operational solar-driven 10-ton LiBr/H<sub>2</sub>O single-effect absorption cooling system in Thailand. *Renew Energy* 2008;33:943–9.
- [24] Ali AHH, Noeres P, Pollerberg C. Performance assessment of an integrated free cooling and solar powered single-effect lithium bromide–water absorption chiller. *Sol Energy* 2008;82:1021–30.
- [25] Monné C, Alonso S, Palacín F, Serra L. Monitoring and simulation of an existing solar powered absorption cooling system in Zaragoza (Spain). *Appl Therm Eng* 2011;31:28–35.
- [26] Rosiek S, Battles FJ. Integration of the solar thermal energy in the construction: Analysis of the solar-assisted air-conditioning system installed in CIESOL building. *Renew Energy* 2009;34:1423–31.

- [27] Ortiz M, Barsun H, He H, Vorobief P, Mammoli A. Modeling of a solar-assisted HVAC system with thermal storage. *Energy Build* 2010;42:500–9.
- [28] Lu ZS, Wang RZ, Xia ZZ, Lu XR, Yang CB, Ma YC, et al. Study of a novel solar adsorption cooling system and a solar absorption cooling system with new CPC collectors. *Renew Energy* 2013;50:299–306.
- [29] Duff WS, Winston R, O'Gallagher JJ, Bergquam J, Henkel T. Performance of the Sacramento demonstration ICPC collector and double effect chiller. *Sol Energy* 2004;76:175–80.
- [30] Lokurlu A, Richarts F, Krüger D. High efficient utilization of solar energy with newly developed parabolic trough collectors (SOLITEM PTC) for chilling and steam production in a hotel at the Mediterranean coast of Turkey. *Int J Energy Technol Policy* 2005;3:137–46.
- [31] Qu M, Yin H, Archer DH. A solar thermal cooling and heating system for a building: experimental and model based performance analysis and design. *Sol Energy* 2010;84:166–82.
- [32] Balghouthi M, Chahbani MH, Guizani A. Investigation of a solar cooling installation in Tunisia. *Appl Energy* 2012;98:138–48.
- [33] Weber C, Berger M, Mehling F, Heinrich A, Núñez T. Solar cooling with water–ammonia absorption chillers and concentrating solar collector – operational experience. *Int J Refrig* 2013;1–20.
- [34] Hu Y, Schaefer L, Hartkopf V. Energy and exergy analysis of integrating compound parabolic collectors (CPC) with lithium bromide (Li–Br) absorption chiller for building heating and cooling to achieve net zero buildings. *pdf. ASHRAE Trans* 2011;117:174–82.
- [35] Bermejo P, Pino FJ, Rosa F. Solar absorption cooling plant in Seville. *Sol Energy* 2010;84:1503–12.
- [36] Streicher W. Laboratory prototypes of PCM storage units. IEA SHC Task 32 Report C3; 2007.
- [37] Gil A, Barreneche C, Moreno P, Solé C, Inés Fernández A, Cabeza LF. Thermal behavior of d-mannitol when used as PCM: comparison of results obtained by DSC and in a thermal energy storage unit at pilot plant scale. *Appl Energy* 2013;111:107–13.
- [38] Gil A, Oró E, Castell A, Cabeza LF. Experimental analysis of the effectiveness of a high temperature thermal storage tank for solar cooling applications. *Appl Therm Eng* 2013;54:521–7.
- [39] Gil A, Oró E, Miró L, Peiró G, Ruiz Á, Salmerón JM, et al. Experimental analysis of hydroquinone used as phase change material (PCM) to be applied in solar cooling refrigeration. *Int J Refrig* 2013;1–9.
- [40] Dincer I, Rosen MA. Thermal energy storage: systems and applications. 2nd ed. The Atrium, Southern Gate, Chichester, West Sussex, United Kingdom: John Wiley & Sons Ltd; 2011.
- [41] Fernandez AI, Martínez M, Segarra M, Martorell I, Cabeza LF. Selection of materials with potential in sensible thermal energy storage. *Sol Energy Mater Sol Cells* 2010;94 (1723–9).
- [42] Basecq V, Michaux G, Inard C, Blondeau P. Short-term storage systems of thermal energy for buildings: a review. *Adv Build Energy Res* 2013;7:66–119.
- [43] Laing D, Steinmann W-D, Tammé R, Richter C. Solid media thermal storage for parabolic trough power plants. *Sol Energy* 2006;80:1283–9.
- [44] Pilkington Solar International GmbH. Survey of thermal storage for parabolic trough power plants. NREL/SR-550-27925; 2000.
- [45] Berndt Wischnewski. Water/steam properties. Peace Softw; 2013.
- [46] (<http://everylittledrop.com.au>). The cost of water; 2014.
- [47] Fernandes D, Pitié F, Cáceres G, Baeyens J. Thermal energy storage: how previous findings determine current research priorities. *Energy* 2012;39:246–57.
- [48] Tatsidjoudoung P, le Pierrès N, Luo L. A review of potential materials for thermal energy storage in building applications. *Renew Sustain Energy Rev* 2013;18:327–49.
- [49] Graeter F, Rheinländer J. Thermische Energiespeicherung mit Phasenwechsel im Bereich von 150 bis 400 °C. In: Proc. ForschungsVerbund Sonnenenergie Work. Wärmespeicherung, Col. Ger., 2001.
- [50] Streicher W, Cabeza LF, Heinz A. Inventory of phase change materials (PCM). IEA SHC Task 32 Report C2; 2005.
- [51] Sugo H, Kisi E, Cuskelly D. Miscibility gap alloys with inverse microstructures and high thermal conductivity for high energy density thermal storage applications. *Appl Therm Eng* 2013;51:1345–50.
- [52] Gil A, Oró E, Peiró G, Álvarez S, Cabeza LF. Material selection and testing for thermal energy storage in solar cooling. *Renew Energy* 2013;57:366–71.
- [53] Kenisarin MM, Mahkamov K. Solar energy storage using phase change materials. *Renew Sustain Energy Rev* 2007;11:1913–65.
- [54] Mehling H, Cabeza LF. Heat and cold storage with PCM—an up to date introduction into the basics and applications. Berlin Heidelberg: Springer; 2008.
- [55] Sharma SD, Sagara K. Latent heat storage materials and systems: a review. *Int J Green Energy* 2005;2:1–56.
- [56] Zalba B, Marin JM, Cabeza LF, Mehling H. Review on thermal energy storage with phase change: materials, heat transfer analysis and applications. *Appl Therm Eng* 2003;23:251–83.
- [57] CRC. Handbook of chemistry and physics Online. 94th ed. n.d.
- [58] Sigma-Aldrich n.d.
- [59] Pincemin S, Olives R, Py X, Christ M. Highly conductive composites made of phase change materials and graphite for thermal storage. *Sol Energy Mater Sol Cells* 2008;92:603–13.
- [60] Kenisarin MM. High-temperature phase change materials for thermal energy storage. *Renew Sustain Energy Rev* 2010;14:955–70.
- [61] (<http://www.infomine.com>). Tin prices 2014.
- [62] Abedin AH, Rosen MA. A critical review of thermochemical energy storage systems. *Open Renew Energy J* 2011;4:42–6.
- [63] Kato Y. Chemical energy conversion technologies for efficient energy use. Paksoy HO NATO science series II. Mathematics physics and chemistry, vol. 234. Thermal energy storage for sustainable energy consumption—Fundamentals, case studies and designs. Dordrecht: Springer; 2007. p. 377–91.
- [64] Cot-Gores J, Castell A, Cabeza LF. Thermochemical energy storage and conversion: a state-of-the-art review of the experimental research under practical conditions. *Renew Sustain Energy Rev* 2012;16:5207–24.
- [65] Bales C. Laboratory tests of chemical reactions and prototype sorption storage units. IEA SHC Task 32 Subtask B report B4; 2008.
- [66] van Essen VM, Bleijendaal LPJ, Kikkert BWJ, Zondag HA, Bakker M, Bach PW. Development of a compact heat storage system based on salt hydrates. In: Proceedings of the international conference on solar heating, cooling for buildings. Graz, Austria; September 28–Oct 1, 2010.
- [67] Bertsch F, Mette B, Asenbeck S, Kerskes H, Müller-Steinhagen H. Low temperature chemical heat storage—an investigation of hydration reactions. In: Proceedings of Effstock; 2009.
- [68] Kuravi S, Trahan J, Goswami DY, Rahman MM, Stefanakos EK. Thermal energy storage technologies and systems for concentrating solar power plants. *Prog Energy Combust Sci* 2013;39:285–319.
- [69] Pinel P, Cruickshank CA, Beausoleil-Morrison I, Wills A. A review of available methods for seasonal storage of solar thermal energy in residential applications. *Renew Sustain Energy Rev* 2011;15:3341–59.
- [70] Rosengarten G, Morrison G, Behnia M. A second law approach to characterising thermally stratified hot water storage with application to solar water heaters. *J Sol Energy Eng* 1999;121:194.
- [71] Rosen MA, Tang R, Dincer I. Effect of stratification on energy and exergy capacities in thermal storage systems. *Int J Energy Res* 2004;28:177–93.
- [72] levers S, Lin W. Numerical simulation of three-dimensional flow dynamics in a hot water storage tank. *Appl Energy* 2009;86:2604–14.
- [73] Han YM, Wang RZ, Dai YJ. Thermal stratification within the water tank. *Renew Sustain Energy Rev* 2009;13:1014–26.
- [74] Viessmann GmbH and Co. KG. Technical guide: solar thermal systems; 2014.
- [75] Viessmann GmbH and Co. KG. viessmann.com; 2014.
- [76] Cabeza LF. Concurrent GI. Thermal energy storage. Comprehensive renewable energy, vol. 3. Universitat de Lleida: Elsevier Ltd.; 2012. p. 211–54.
- [77] Al-Marafie A, Moustafa SM, Al-Kandarie A. Factors affecting static stratification of thermal water storage. *Energy Sources* 1989;11:183–99.
- [78] Streicher W, Bales C. Combistores. In: Hadorn J, editor. Therm. Energy Storage Sol. Low Energy Build. Spain: Universitat de Lleida; 2005. p. 29–40.
- [79] Spur R, Fiala D, Nevralla D, Probert D. Performances of modern domestic hot-water stores. *Appl Energy* 2006;83:893–910.
- [80] Youssef Z, Delahaye A, Huang L, Trinquet F, Fournaison L, Pollerberg C, et al. State of the art on phase change material slurries. *Energy Convers Manag* 2013;65:120–32.
- [81] Nallusamy N, Sampath S, Velraj R. Experimental investigation on a combined sensible and latent heat storage system integrated with constant/varying (solar) heat sources. *Renew Energy* 2007;32:1206–27.
- [82] Trp A, Lenic K, Frankovic B. Analysis of the influence of operating conditions and geometric parameters on heat transfer in water-paraffin shell-and-tube latent thermal energy storage unit. *Appl Therm Eng* 2006;26:1830–9.
- [83] Esen M, Ayhan T. Development of a model compatible with solar assisted cylindrical energy storage tank and variation of stored energy with time for different phase change materials. *Energy Convers Manag* 1996;37:1775–85.
- [84] Mehling H, Cabeza LF, Hippeli S, Hiebler S. PCM-module to improve hot water heat stores with stratification. *Renew Energy* 2003;28:699–711.
- [85] Cabeza LF, Ibáñez M, Solé C, Roca J, Nogués M. Experimentation with a water tank including a PCM module. *Sol Energy Mater Sol Cells* 2006;90:1273–82.
- [86] Calmac. CALMAC Manufacturing Corp.; 2013.
- [87] Medrano M, Yilmaz MO, Nogués M, Martorell I, Roca J, Cabeza LF. Experimental evaluation of commercial heat exchangers for use as PCM thermal storage systems. *Appl Energy* 2009;86:2047–55.
- [88] Helm M, Keil C, Hiebler S, Mehling H, Schweigler C. Solar heating and cooling system with absorption chiller and low temperature latent heat storage: energetic performance and operational experience. *Int J Refrig* 2009;32: 596–606.
- [89] Shamsundar N, Srinivasan R. Analysis of energy storage by phase change with an array of cylindrical tubes. In: Thermal storage and heat transfer in solar energy systems; proceedings of the winter annual meeting. San Francisco California; December 10–15, 1978 (A79-26201 09-44), New York: American Society of Mechanical Eng; 1978. p 35–40.
- [90] Asgarpour S. Heat transfer in laminar flow with a phase change boundary. *J Heat Transfer* 1982;104:678–82.
- [91] Saxena S. A preliminary model for phase change thermal energy storage in a shell and tube heat exchanger. *Sol Energy* 1982;29:257–63.
- [92] Lacroix M. Numerical simulation of a shell-and-tube latent heat thermal energy storage unit. *Sol Energy* 1993;50:357–67.
- [93] Hoffmann J. Prediction of shell and tube thermal energy store performance. In: Proceedings of the intersociety energy conversion engineering conference, vol. 2; 1995. p. 249–57.
- [94] Gong Z-X. Finite-element analysis of cyclic heat transfer in a shell-and-tube latent heat energy storage exchanger. *Appl Therm Eng* 1997;17:583–91.
- [95] Longeon M, Soupart A, Fournigüé J-F, Bruch A, Marty P. Experimental and numerical study of annular PCM storage in the presence of natural convection. *Appl Energy* 2013;112:175–84.

- [96] Jegadheeswaran S, Pohekar SD. Performance enhancement in latent heat thermal storage system: a review. *Renew Sustain Energy Rev* 2009;13:2225–44.
- [97] Regin aF, Solanki SC, Saini JS. Heat transfer characteristics of thermal energy storage system using PCM capsules: a review. *Renew Sustain Energy Rev* 2008;12:2438–58.
- [98] Oró E, Gil A, Miró L, Peiró G, Álvarez S, Cabeza LF. Thermal energy storage implementation using phase change materials for solar cooling and refrigeration applications. *Energy Procedia* 2012;30:947–56.
- [99] Buchlin JM. Experimental and numerical modeling of solar energy storage in rockbeds and encapsulated phase change packings. In: Kilikis B, Kakac S, editors. *Energy Storage Syst.* NATO ASI S. Kluwer Academic Publishers; 1989. p. 249–301.
- [100] Bédécarrats J, Strub F, Falcon B, Dumas J. Phase-change thermal energy storage using spherical capsules: performance of a test plant. *Int J Refrig* 1996;19:187–96.
- [101] Wu S, Fang G. Dynamic performances of solar heat storage system with packed bed using myristic acid as phase change material. *Energy Build* 2011;43:1091–6.
- [102] ElGhnam RI, Abdelaziz RA, Sakr MH, Abdelrhman HE. An experimental study of freezing and melting of water inside spherical capsules used in thermal energy storage systems. *Ain Shams Eng J* 2012;3:33–48.
- [103] Aldoss T. Latent solar thermal storage systems: packed beds with spherical phase change capsules of different physicochemical properties. In: *Proceedings of the 7th international ASME Conference on energy sustainability*. Minneapolis, Minnesota, USA: ASME; 2013. p. V001T09A003.
- [104] Ereke A, Ilken Z, Acar MA. Experimental and numerical investigation of thermal energy storage with a finned tube. *Int J Energy Res* 2005;29:283–301.
- [105] Akgün M, Aydın O, Kaygusuz K. Thermal energy storage performance of paraffin in a novel tube-in-shell system. *Appl Therm Eng* 2008;28:405–13.
- [106] Chaxiu G., Hexin D., Xinli W. Performance enhancement of a PCM cold storage under condition of heat flux. 2010 In: *Proceedings of the international conference on challenges in environmental science and computer engineering*; 2010. p. 499–502.
- [107] Nithyanandam K, Pitchumani R. Analysis and optimization of a latent thermal energy storage system with embedded heat pipes. *Int J Heat Mass Transf* 2011;54:4596–610.
- [108] Ezan MA, Ozdogan M, Ereke A. Experimental study on charging and discharging periods of water in a latent heat storage unit. *Int J Therm Sci* 2011;50:2205–19.
- [109] Jegadheeswaran S, Pohekar SD, Kousksou T. Conductivity particles dispersed organic and inorganic phase change materials for solar energy storage—an exergy based comparative evaluation. *Energy Proc* 2012;14:643–8.
- [110] Nithyanandam K, Pitchumani R. Computational studies on a latent thermal energy storage system with integral heat pipes for concentrating solar power. *Appl Energy* 2013;103:400–15.
- [111] Tay NHS, Bruno F, Belusko M. Experimental investigation of dynamic melting in a tube-in-tank PCM system. *Appl Energy* 2013;104:137–48.
- [112] Avci M, Yazici MY. Experimental study of thermal energy storage characteristics of a paraffin in a horizontal tube-in-shell storage unit. *Energy Convers Manag* 2013;73:271–7.
- [113] Parry AJ, Eames PC, Agyenim F. Modeling of thermal energy storage shell-and-tube heat exchanger. *Heat Transf Eng* 2014;35:1–14.
- [114] Gil A, Medrano M, Martorell I, Lázaro A, Dolado P, Zalba B, et al. State of the art on high temperature thermal energy storage for power generation. Part 1—Concepts, materials and modellization. *Renew Sustain Energy Rev* 2010;14:31–55.
- [115] Medrano M, Gil A, Martorell I, Potau X, Cabeza LF. State of the art on high-temperature thermal energy storage for power generation. Part 2—case studies. *Renew Sustain Energy Rev* 2010;14:56–72.
- [116] Siegel NP. Thermal energy storage for solar power production. *Wiley Interdiscip Rev Energy Environ* 2012;1:119–31.
- [117] Eck M. Thermal storage for STE Plants. In: *3rd SFERA Summer Sch.* Almer; June 27–28, 2012.
- [118] Flueckiger SM, Yang Z, Garimella SV. Review of molten-salt thermocline tank modeling for solar thermal energy storage. *Heat Transf Eng* 2013;34:787–800.
- [119] Tian Y, Zhao CY. A review of solar collectors and thermal energy storage in solar thermal applications. *Appl Energy* 2013;104:538–53.
- [120] Steinmann W-D, Eck M. Buffer storage for direct steam generation. *Sol Energy* 2006;80:1277–82.
- [121] Pacheco JE. Final test and evaluation results from the solar two project; 2002.
- [122] Herrmann U, Kelly B, Price H. Two-tank molten salt storage for parabolic trough solar power plants. *Energy* 2004;29:883–93.
- [123] SolarPaces. Concentrating solar power from research to implementation; 2007.
- [124] NREL. Solar Electric Generating Station I; 2009 n.d.
- [125] Tamme R. Concrete storage: update on the German concrete TES program. *Work. therm. storage trough power syst.. Golden CO: Inst. Tech. Thermodyn*; 2003.
- [126] Henning H-M. Solar assisted air conditioning of buildings – an overview. *Appl Therm Eng* 2007;27:1734–49.
- [127] Sonntag C, Ding H, Engell S. Supervisory control of a solar air conditioning plant with hybrid dynamics. *Eur J Control* 2008;14:451–63.
- [128] Kohlenbach P. Solar cooling with absorption chillers: control strategies and transient chiller performance. *Technical University of Berlin*; 2006.
- [129] Bujedo LA, Rodríguez J, Martínez PJ. Experimental results of different control strategies in a solar air-conditioning system at part load. *Sol Energy* 2011;85:1302–15.
- [130] Klein SA. Calculation of flat-plate collector utilizability. *Sol Energy* 1978;21:393–402.
- [131] Rosiek S, Batlles FJJ. Reducing a solar-assisted air-conditioning system's energy consumption by applying real-time occupancy sensors and chilled water storage tanks throughout the summer: A case study. *Energy Convers Manag* 2013;76:1029–42.
- [132] Li Z, Sumathy K. Experimental studies on a solar powered air conditioning system with partitioned hot water storage tank. *Sol Energy* 2001;71:285–97.
- [133] Pasamontes M, Álvarez JDD, Guzmán JLL, Berenguel M, Camacho EFF. Hybrid modeling of a solar-thermal heating facility. *Sol Energy* 2013;97:577–90.
- [134] García CE, Prett DM, Morari M. Model predictive control: Theory and practice – a survey. *Automatica* 1989;25:335–48.
- [135] Mammoli A, Stadler M, Deforest N, Barsun H, Burnett R, Marnay C, et al. Software-as-a-Service optimised scheduling of a solar-assisted HVAC system with thermal storage. In: *Proceedings of the 3rd international conference on microgeneration related technologies*, vol. 11231; 2013.
- [136] Rodríguez M, de Prada C, Capraro F, Cristea S. Logic Embedded NMPC of a Solar Air Conditioning Plant. *Eur J Control* 2008;14:484–500.
- [137] Zambrano D, García-Gabín W. Hierarchical control of a hybrid solar air conditioning plant. *Eur J Control* 2008;14:464–83.
- [138] Menchinelli P, Bemporad A. Hybrid model predictive control of a solar air conditioning plant. *Eur J Control* 2008;14:501–15.
- [139] Fedrizzi R, Franchini G, Mugnier D, Melograno PN, Theofilidi M, Thuer A., et al. Assessment of standard small-scale solar cooling configurations within the solarcombi+ project. In: *Proceedings of the 3rd international conference on solar air-conditioning*. Palermo: OTTI, Renewable Energies; 2009.
- [140] Henning H-M. Comparison of solar thermal versus PV in buildings—an example. In: *IEA SHC Task 38–9th Expert Meeting*. Graz, Austria; 2010.
- [141] IEA, SHC Task 38 solar air-conditioning and refrigeration Subtask A: pre-engineered systems for residential and small commercial applications; 2011.
- [142] Kalogirou SA. Optimization of solar systems using artificial neural-networks and genetic algorithms. *Appl Energy* 2004;77:383–405.
- [143] Vidal H, Colle S, Pereira GDS. Modeling and hourly simulation of a solar ejector cooling system. *Appl Therm Eng* 2006;26:663–72.
- [144] Tsoutsos T, Aloumpi E, Gkouskos Z, Karagiorgas M. Design of a solar absorption cooling system in a Greek hospital. *Energy Build* 2010;42:265–72.
- [145] Calise F, Palombo A, Vanoli L. Maximization of primary energy savings of solar heating and cooling systems by transient simulations and computer design of experiments. *Appl Energy* 2010;87:524–40.
- [146] Hang Y, Du L, Qu M, Peeta S. Multi-objective optimization of integrated solar absorption cooling and heating systems for medium-sized office buildings. *Renew Energy* 2013;52:67–78.
- [147] Arkar C, Vidrih B, Medved S. Efficiency of free cooling using latent heat storage integrated into the ventilation system of a low energy building. *Int J Refrig* 2007;30:134–43.
- [148] El Qarnia H. Numerical analysis of a coupled solar collector latent heat storage unit using various phase change materials for heating the water. *Energy Convers Manag* 2009;50:247–54.
- [149] Padovan R, Manzan M. Genetic optimization of a PCM enhanced storage tank for solar domestic hot water systems. *Sol Energy* 2014.
- [150] Kohlenbach P, Ziegler F. A dynamic simulation model for transient absorption chiller performance. Part II: numerical results and experimental verification. *Int J Refrig* 2008;31:226–33.
- [151] Noro M, Lazzarin RM, Busato F. Solar cooling and heating plants: an energy and economic analysis of liquid sensible vs phase change material (PCM) heat storage. *Int J Refrig* 2013;39:1–13.